



1 **The 1538 eruption at Campi Flegrei resurgent caldera: implications for future unrest and**
2 **eruptive scenarios**

3 **Giuseppe Rolandi¹, Claudia Troise², Marco Sacchi³, Massimo di Lascio⁴, Giuseppe De Natale²**

4 ¹ Università di Napoli Federico II, Dept. Earth Sciences, Naples (I)

5 ² Istituto Nazionale di Geofisica e Vulcanologia, Osservatorio Vesuviano, Naples (I)

6 ³ ISMAR-CNR, Naples (I)

7 ⁴ Free Lance Geologist, Naples (I)

8 Corresponding author: Giuseppe De Natale, giuseppe.denatale@ingv.it

9

10

11 Abstract

12 The recent unrest in the Campi Flegrei caldera which began several decades ago, poses a high risk to
13 a densely populated area, due to significant uplift, very shallow earthquakes of intermediate
14 magnitude and the potential for an eruption. Given the high population density, it is crucial, especially
15 for civil defense purposes, to consider realistic scenarios for the evolution of these phenomena,
16 particularly seismicity and potential eruptions. The eruption of 1538, the only historical eruption in
17 the area, provides a valuable basis for understanding how unrest episodes in this caldera may evolve
18 toward an eruption. In this paper, we provide a new historical reconstruction of the precursory
19 phenomena of the 1538 eruption, analyzed considering recent volcanological observations and results
20 obtained in the last few decades. This allows us to build a coherent picture of the mechanism and
21 possible evolution of the present unrest, including expected seismicity, ground uplift and eruptions.
22 Our work identifies two main alternative scenarios, providing a robust guideline for civil protection
23 measures, and facilitating the development of effective emergency plans in this highly risky area.

24 **1. Introduction**

25 The Campi Flegrei area has been a benchmark of modern geology and volcanology since the middle
26 XVIII century, due to the clear evidence of significant ground movements, associated with both uplift
27 and subsidence, imprinted on the columns of the ancient Roman Market (Macellum) in the town of
28 Pozzuoli. These movements were famously depicted on the cover of Charles Lyell's seminal book,
29 'Principles of Geology'.. By the XIX century, it became evident that the impressive relative



30 movements between sea level and ground were due to ground uplift and subsidence. Consequently,
31 numerous efforts have been made to reconstruct the timeline of these movements, during the
32 centuries,. One of the most convincing reconstructions was proposed by Parascandola (1947), later
33 modified by Dvorak and Mastrolorenzo (1991), Morhange et al. (2006), Bellucci et al. (2006) and,
34 more recently, Di Vito et al. (2016). However, all these reconstructions exhibit evident discrepancies,
35 and do not rely on the full body of historical evidence, as we will demonstrate. These significant
36 ground movements have predominantly involved a long-term trend of subsidence, punctuated by
37 occasional episodes of rapid ground uplift, culminating in the only eruption occurred in historical
38 times, in 1538 (Di Vito et al., 2016). After the 1538 eruption, a new period of subsidence began,
39 which was interrupted in 1950, when a new series of uplift episodes commenced (Del Gaudio et al.,
40 2010). Two major uplift episodes occurred between 1969-1972 and 1982-1984, characterized by
41 significant and rapid uplift (with a cumulative uplift of about 3.5 m) accompanied by intense
42 seismicity. These events led to the evacuation of 3000 residents from the oldest part of Pozzuoli town
43 (Rione Terra), in 1970, and the entire town of Pozzuoli comprising 40.000 people, in 1984 (Barberi
44 et al., 1984). After approximately 20 years of subsidence, a new uplift phase began in 2005-2006,
45 with a much lower uplift rate (0.01 meters per month on average, compared to about 0.06 meters per
46 month in the 1970s and 1980s), but long-lasting and still ongoing. This new unrest has been
47 accompanied by progressively increasing seismicity, which has substantially intensified, both in
48 frequency and maximum magnitude. The maximum magnitude reached $M=4.4$ on May 20, 2024,
49 once the maximum ground level attained at the end of 1984 was reached (in July 2022) and surpassed.
50 The progressively increasing seismicity confirms the predictions of Kilburn et al. (2017) and Troise
51 et al. (2019), who based their forecast on the correspondence of the ground level with stress levels at
52 depth. This seismic activity represents a significant and continuous hazard for the edifices in such a
53 densely populated area, given the very shallow depth of the earthquakes (about 2-3 km). Furthermore,
54 the current crisis poses an even higher threat as it could potentially be a precursor to a future eruption
55 in the area.

56 The present study is aimed to reconstruct and interpret the events before and after the 1538 eruption.
57 This analysis follows three main paths: i) the accurate reconstruction, of the ground movements in
58 this area since early historical times, using historical testimonies and documentation; ii) the accurate
59 reconstruction of the uplift movements that evolved from 1430 to 1538, accompanied and followed
60 by significant seismic events; iii) the analysis of stratigraphic and geophysical parameters, which,
61 although collected in the recent era, provide important elements for the reconstruction and
62 interpretation of the unrest related to the 1538 eruption.

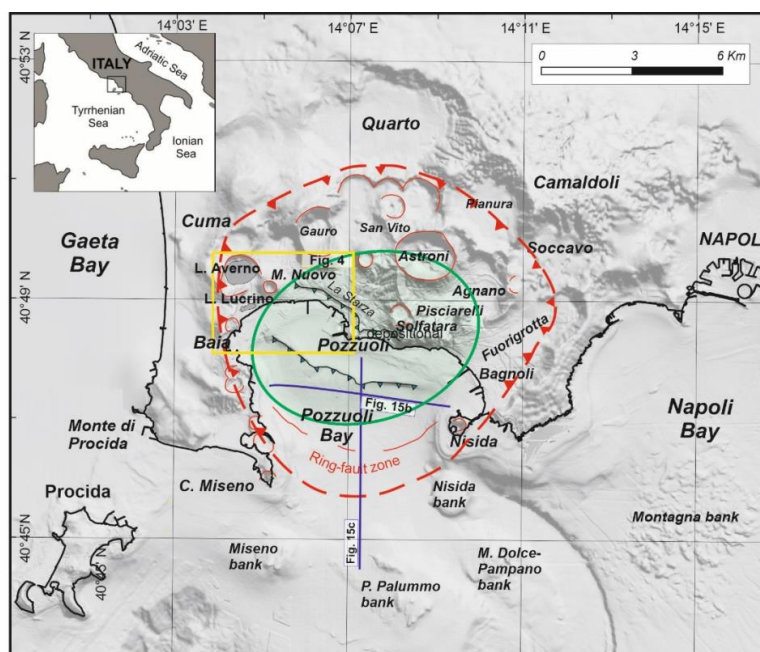


63 Finally, the interpretation of the events preceding, accompanying and following the 1538 eruption is
64 used to provide insight into possible evolution scenarios for the present unrest, which started in 1950
65 and is still in progress (Troise et al., 2019; Scarpa et al., 2022)

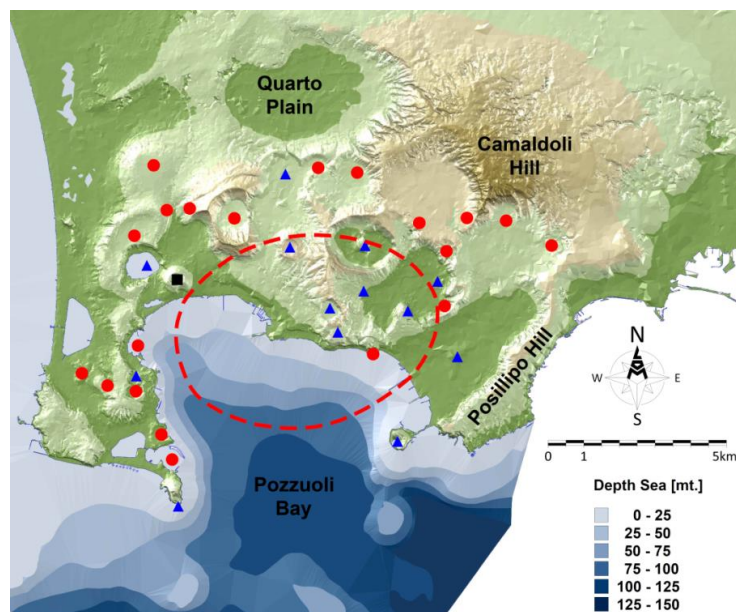
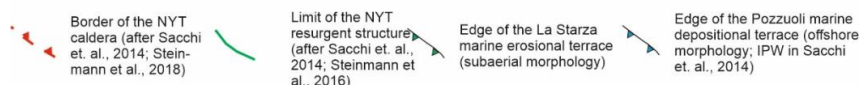
66

67 **2. Caldera formation and post-caldera volcanic activity 14 ka - 3.7 ka**

68 Campi Flegrei caldera has been generated by a huge eruptive event, the 15 ka Neapolitan
69 Yellow Tuff (NYT), as demonstrated by recent research based on drilling results (Rolandi
70 et al., 2020a; 2020b). The caldera collapse resulted in many new fractures, which gradually
71 became eruptive vents. Through these vents, the eruptions continued, exhibiting the
72 characteristics of a volcanic field (Druitt and Sparks, 1984), resulting in the so-called post-
73 caldera activity. Dome-shaped uplift of NYT occurred after the caldera formation in the
74 central zone of Campi Flegrei, with uplift up to hundreds of meters on the caldera floor (Rolandi
75 et al., 2020b). The significant uplift involved a large intra-calderic NYT block, making Campi Flegrei
76 a typical example of resurgent caldera (Rolandi et al., 2020b). The post-caldera activity gave rise
77 to numerous craters, predominantly tuff cones and tuff rings (Fig. 1a,b), displaying the
78 typical characters of monogenic volcanoes (Marti et al., 2016). Within Campi Flegrei, 35
79 small eruptive centers have been identified, since the NYT eruption (Di Vito et al., 1999;
80 Smith et al., 2012), producing more than 60 eruptions. The magmas associated with these
81 eruptions are typically trachytes and alkali trachytes, with smaller amounts of latite and
82 phonolite (Di Girolamo et al., 1984; Rosi and Sbrana, 1987; D'Antonio et al., 1999). The
83 post-caldera eruptions can be then classified in two periods, occurring between 14 ka
84 and 8.2 ka BP and 5.8 and 3.7 ka BP., respectively, with an interval of significant
85 subsidence without eruptions from 8.2 to 5.8 ka BP (Rolandi et al., 2020b).



86



87

88 **Fig. 1 – Top:** Location map of the study area with indication of relevant toponyms and
 89 major volcano-tectonic and morpho-structural lineaments associated with the Campi
 90 Flegrei caldera. **Bottom:** Map of Campi Flegrei caldera. Red circles indicate the craters of
 91 the first post-caldera volcanic phase, blue triangles indicate the craters of the second phase.
 92 The red hatched area represents the resurgent block of NYT extended in the Pozzuoli Bay.



93

94 The second post-caldera eruptive phase was preceded by the uplift of 30m, above sea
95 level, of La Starza marine terrace (Cinque et al., 1983; Rolandi et al., 2020b). The
96 distribution of eruptive centers reveals that, during the first post-caldera phase, they were
97 distributed around the resurgent block. In the second phase, among thirteen volcanic edifices,
98 seven occurred within the resurgent area (Fig. 1).

99 It seems likely that the second post-caldera phase (5.8 - 3.7 ka) can be considered the primary
100 reference for defining possible future eruptive scenarios, following the eruption of 1538 AD.

101

102 **3. Subsidence and uplift evolution before the 1538 eruption**

103 As inferred from historical chronicles, as well as from studies on the incrustations and traces of
104 bioerosion on the Pozzuoli Serapeum marble columns (Parascandola 1947; Bellucci et al. 2006), after
105 the two post-caldera phases previously defined, large ground uplift and subsidence in the order of
106 tens of meters, occurred. Historical documents allowed us to precisely reconstruct such ground
107 movements in Pozzuoli area (central part of the caldera) and in the Averno area (3 km west of
108 Pozzuoli, close to the area where the 1538 eruption occurred. The reconstruction reported here, based
109 on all reliable historical documents, is the most complete and rigorous, correcting several
110 misinterpretations and/or erroneous reconstructions that appeared in previous literature.

111 The first evidence of subsidence in the Campi Flegrei area dates back Greek times, as reported by
112 Diodoro Siculo (VIII century BC) and is related to the area in front of the Averno Lake, and the 1538
113 eruption which generated the Monte Nuovo cone. We will start to describe the historical documents
114 to shed light on the ground movements in this area, then we will reconstruct ground movements in
115 the most deformed, central Pozzuoli area.

116 A fundamental historical marker for inferring the ground movements west of Pozzuoli, is the Via
117 Herculea, which has been used since the Greek times (beginning in the 8th century BC) and continued
118 to be very important during the Roman times. Via Herculea, whose detailed history is shown in the
119 supplementary material for a reconstruction of its movements as reported by several sources during
120 the past centuries, was the name given to a road running on a thin land strip, likely formed by
121 aggradation in coastal shallow water settings of volcanoclastic sandy deposits (Parascandola, 1943),
122 mostly erupted from the 5ka and 3.7 ka eruptions of the Averno and Capo Miseno volcanoes (Sacchi
123 et al., 2014; Di Vito et al. 2011; Di Girolamo et al., 1984), giving rise to a Lake (Fig. 2a). Since the
124 elevation of this land, used as a road running along the coast from Pozzuoli to Baia, was only few
125 meters above the sea level, ground subsidence strongly perturbed its use as a road, and such troubles



126 were often reported in historical documents. For this reason, it provides compelling evidence for the
127 evolution of ground subsidence in this area during the centuries.

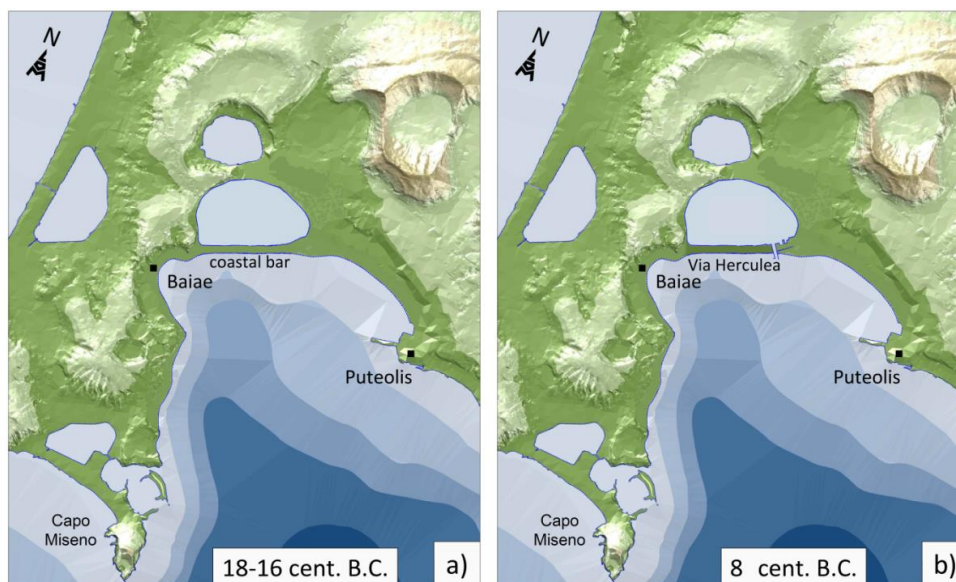
128 The Greeks coming from Euboea in the 8th century BC, firstly settled on the island of Ischia
129 (Pithecusa), then founded the polis of Cuma, which represents the first Greek colony of Magna
130 Graecia and of the entire western Mediterranean. Thus, since the 8th century BC the thin land stipe
131 assumed the function of a road taking the name of Via Herculea, to reach the cultivated countryside
132 around Pozzuoli (Fig. 2b). Diodoro Siculo (see Appendix 1) reported that, already at their times,
133 continuous subsidence affected this area, thus generating problems to the practicability of Via
134 Herculea.

135 In Roman times, since the beginning of the 1st century BC, the body of water enclosed by the Via
136 Herculea, purchased by Sergio Orata, played an important role in fish-farming since 90 BC, taking
137 the name of Lucrino, much larger than the present-day Lake Lucrino. After his death, due to
138 continuous subsidence which menaced both the practicability of the Via Herculea and the fish farming
139 activities, the new owners around 60 BC, turned to the Roman Senate calling for appropriate
140 interventions. For this purpose, in 59 BC Julius Caesar was commissioned, which built a barrier (*Opus*
141 *Pilarum*) and special shutters to protect the road and the Lucrino Lake from sea ingressions (see
142 Appendix 1). Towards the end of the same century, for military purposes, in 37 BC Agrippa cut both
143 the Via Herculea and the barrier with the crater of Avernus. Having understood, unlike Julius Caesar,
144 the continuous subsidence of the Via Herculea, which at the end of the century was only few meters
145 above sea level (Fig. 2c), also **increased its height** (Strabo, 1st century BC). About four centuries later
146 Theodoric (King of the Ostrogoths), upon request for the protection of fish farming, restored the dam
147 by increasing again the height of via Herculea with respect to the sea level (Parascandola, 1943).

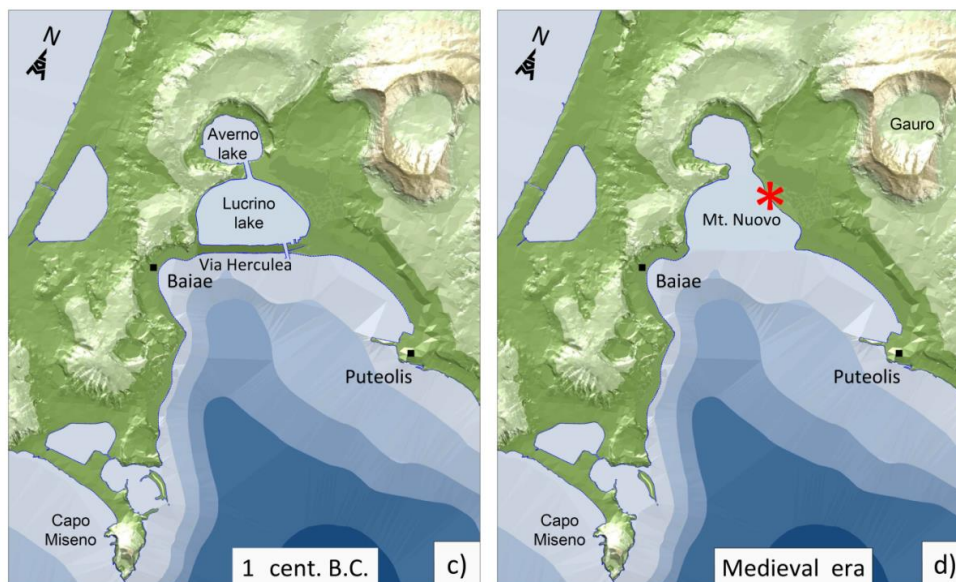
148 Due to continuous subsidence, the Via Herculea finally sank below the sea level between 6th - 7th
149 century A.D, when the sea penetrated the crater of Averno, the Lake Lucrino having disappeared (Fig.
150 2d). Proof of the disappearance of the Via Herculea and of the Lucrino Lake was also testified by
151 Boccaccio, who lived in the Naples area from 1327 to 1341 AD and described the Averno area in its
152 geographical book 'De montibus' (...to Avernus, connected in ancient times with the nearby lake
153 *Lucrino where it recalls the waters of portus Iulius*).



154



155



156 **Fig. 2 - a,b,c,d) position of the via Herculea in relation to the bradiseismic phases along 33**
157 **centuries. The red dot indicates the central point around which the volcanic edifice of 1538 was**
158 **formed.**

159

160 Via Herculea never rose above the sea level again, despite the large uplift phase, occurred before and
161 during the 1538 eruption (see Fig. 2d).



162 The tentative reconstruction of the level of Via Herculea, approximately shown in Fig. 2 as briefly
 163 described above, is shown in detail in Fig. 3, where each point of the curve refers to a specific
 164 documented historical period, starting from the Greek age (8th century BC), through the Roman era
 165 and the late Middle Ages, until the eruptive event of 1538 (see Appendix 1). Note that on the Via
 166 Herculea, at the end of the 1st century BC and at the end of the 4th century AD, works were carried
 167 out to increase its height above sea level due to the incipient submersion. Due to these works,
 168 the submersion of the structure was delayed from ca. the 3rd, 4th century BC, up to the 7th century AD
 169 (Fig. 3). The date of submersion around 6-7th century is also consistent with the observations reported
 170 by Parascandola (1943), indicating that the land strip of Via Herculea still emerged above sea level
 171 for much of the 6th century.

172 It is fundamental to note is that Via Herculea never reemerged again, not even immediately before
 173 and during the eruptive phase of 1538 (Parascandola, 1943).

174 The submerged relicts of the Via Herculea are still visible today located at about 4.5 meters bsl, as
 175 shown in the high-resolution bathymetry (Fig.4) recently obtained by Somma et al. (2016).

176

177

178

179

180

181

182

183

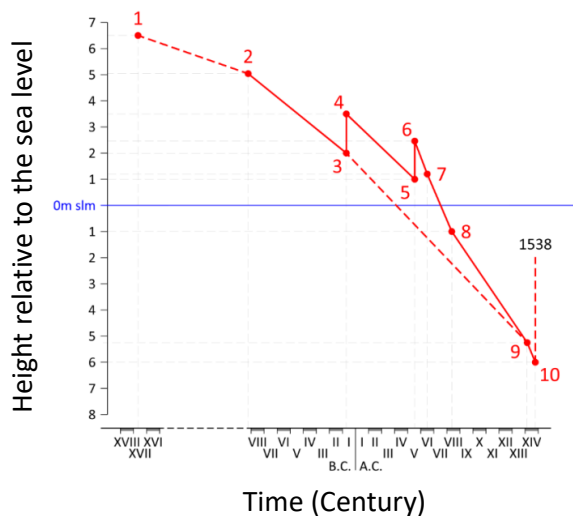
184

185

186

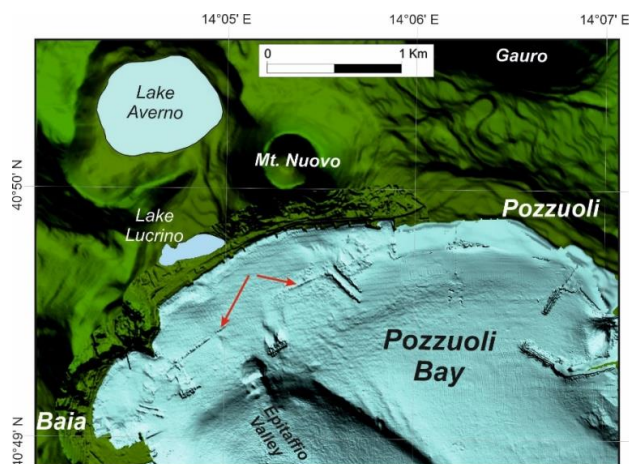
187

188



189 **Fig. 3 – Diagram showing the trend of ground movements at the Via Herculea, as referred to sea level,**
 190 **along 33 centuries.**

191



192

193 **Fig. 4 – Shaded relief map of the coastal area of the Pozzuoli Bay based on high resolution**
194 **multibeam bathymetry (Somma et al., 2016). Arrows indicate the submerged remains of the**
195 **breakwater pilae of the via Herculea.**

196

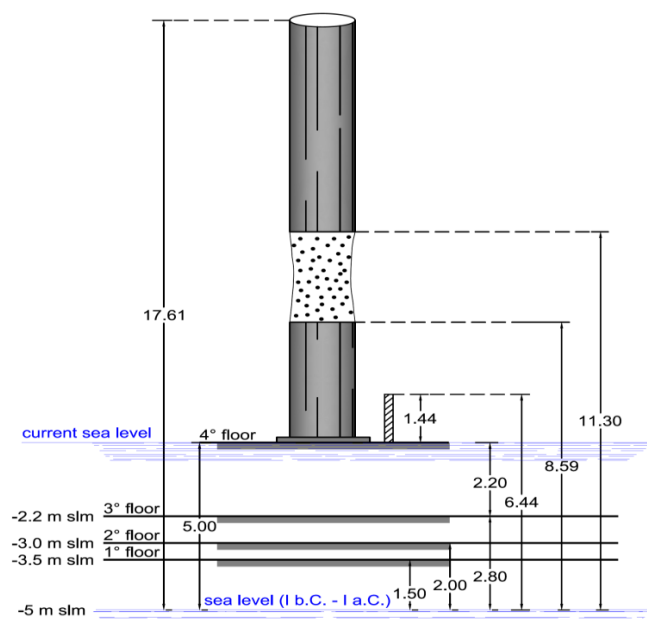
197 Meanwhile Via Herculea records the most ancient subsidence in the whole area, the best evidence for
198 subsidence in the Pozzuoli area, where maximum ground movements are recorded, comes from the
199 historical-archaeological elements linked to the Serapis Temple (Serapeum), although subsidence in
200 the Pozzuoli area is also testified since Greek times (Gauthier, 1912).

201 Recently, Amato and Gialanella (2013) discovered, by drilling into Serapeum area, four successively
202 superimposed floors, ranging from the Augustan age (31 BC-14 AD) to that of the Severi (193-235
203 AD), thus indicating the progressive subsidence of the manufact (Fig. 5). The most elevated 4th floor,
204 was built in the Severi Age, indicating at that time the previously built three floors where all below
205 the sea level, and from this epoch we will follow the historical traces of further subsidence and
206 subsequent uplift. The resulting time evolution of the approximate level of the 4th floor of the
207 Serapeum is reported in Fig. 6. Also in this figure, as for the Fig.4, each number refers to a given
208 historical document supporting that level (see supplementary material, Appendix 2). From historical
209 information we know that the 4th floor subsided below the sea level in the 5th century, i.e., about 200
210 years after its construction during the Severi Age. When the 4th floor reached a level of 3.6 m bsl,
211 around the 7th century AD, the columns were wrapped by layers of sedimentary materials, which
212 formed the so-called "fill" (Parascandola, 1947). Then, due to the impact of the relative sea-level
213 change on the coastal area colonies of lithodomes attached the part of column at the mean sea level,
214 between 3.6 and 6.30 water depth (see the two red arrows in Fig. 7c) and creating a pitted band above
215 the sedimentary materials, for a thickness of 2.70m. This process occurred until the 9th century AD,
216 when the fourth floor located to a depth 6.3 m below sea. Such a depth was considered by some



217 authors (Parascandola 1947, Amato and Gialanella, 2013) to be the maximum submersion reached in
 218 the 9-10th century. In the same period, however, the ground subsidence caused the flooding by
 219 thermal and rain waters, of the Agnano plain, an area located to east of Pozzuoli, and resulted in the
 220 formation of a lake (Annechino, 1931). This event indicated a general persistence of subsidence in
 221 the Pozzuoli area, which was in fact confirmed very clearly even in the following centuries, as
 222 highlighted by numerous historical documents, resumed here (Fig. 7a) and reported in detail in
 223 Appendix 2.

224



225

226 **Fig. 5 – Floors underlying columns of Serapeo (redrawn from Amato and Gialanella, 2013).**

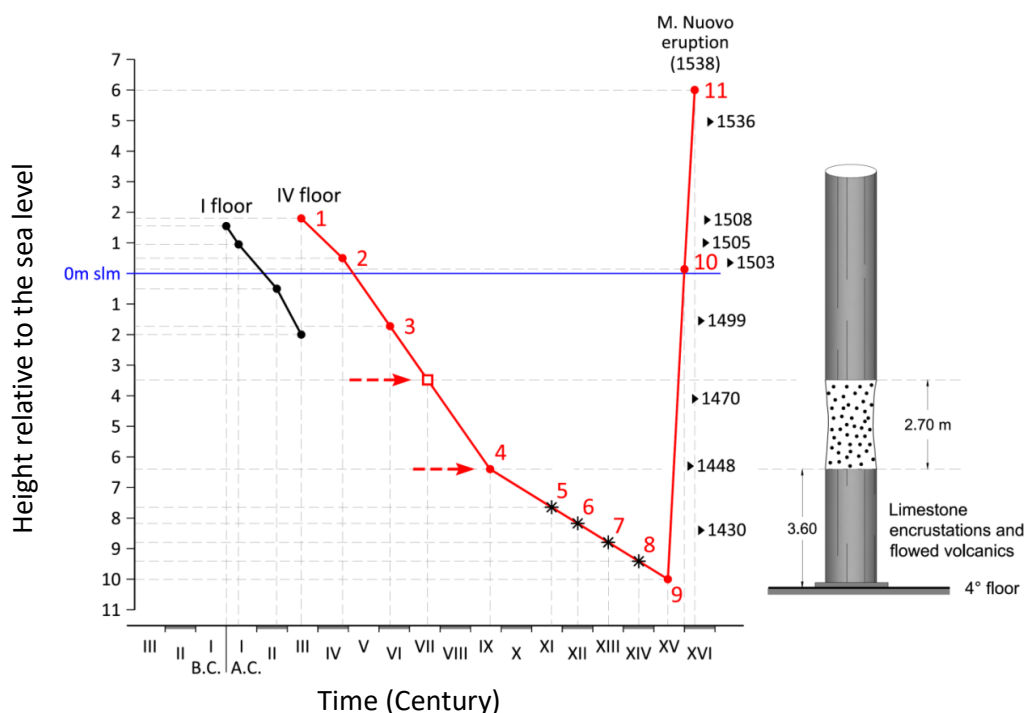
227 **The dotted part of the column indicates the boring due to colonies of *Lithodomus Litophagus*.**

228

229 In the 11th century the Arab geographer Idrisi and other historians of 12th century (Benjamin ben
 230 Yonah de Tudela) and 13th century (Nicolò Jamsilla), clearly highlighted the morphology of Rione
 231 Terra as a medieval castle surrounded by the sea on three sides, due to the continuation of the
 232 subsidence, which was still underway at that time (Costa et al., 2022) (see points 6 and 7 in Appendix
 233 2). Moreover, in 15th century there is the account of Boccaccio (1348), as reported by Parascandola
 234 (1943), who wrote that the fisherman’s wharf in the Bay of Pozzuoli became completely submerged
 235 (point 8 in Appendix 2).



236 We can prove again the subsidence continued further in the following century, since it is possible to
 237 get a more precise estimate of the depth below sea level reached by the 4th floor of the Serapeum, by
 238 observing the painting “Bagno del Cantariello” (Fig. 7a), part of the famous Balneis Puteolanis of the
 239 Edinburgh Codex of 1430 AD (Di Bonito & Giamminelli, 1992). The painting depicts the Rione
 240 Terra encircled by vertical yellow tuff walls, from which the beach of Marina Della Postierla extends
 241 (towards the observer) to the base of the S. Francesco hill, the source of the thermal spring Cantariello
 242 (foreground) near the coast northeast of the submerged Serapeum. Behind the visitors of the thermal
 243 spring, the painting clearly shows the upper part of the three marble columns of Serapeum emerging
 244 from the sea. Also depicted are people fishing directly from the shore (Fig. 7b). From this painting
 245 we can make a roughly estimate of the portion of columns below the sea level at that time, taking in
 246 account that significant part of the columns is submerged. Historical records from the 1750
 247 excavations, (see further) indicate that the buried part of the columns amounted to about 10 m (see
 248 Parascandola, 1947); the shallowest 2 meters of the excavations were formed by pyroclastic flow
 249 deposits of the 1538 eruption 8 (see further paragraphs).



250

251

252 **Fig. 6 – Diagram of ground deformations with reference to the fourth floor of the Serapeo**
 253 **(points 1-4). Points 5-7 indicate the submersion of the Pozzuoli area through the topographic-**
 254 **morphological variations acquired by the Rione Terra due to submersion (see supplementary**
 255 **historical material). Finally, points 8-9 indicate the extent of the submersion referring to the**

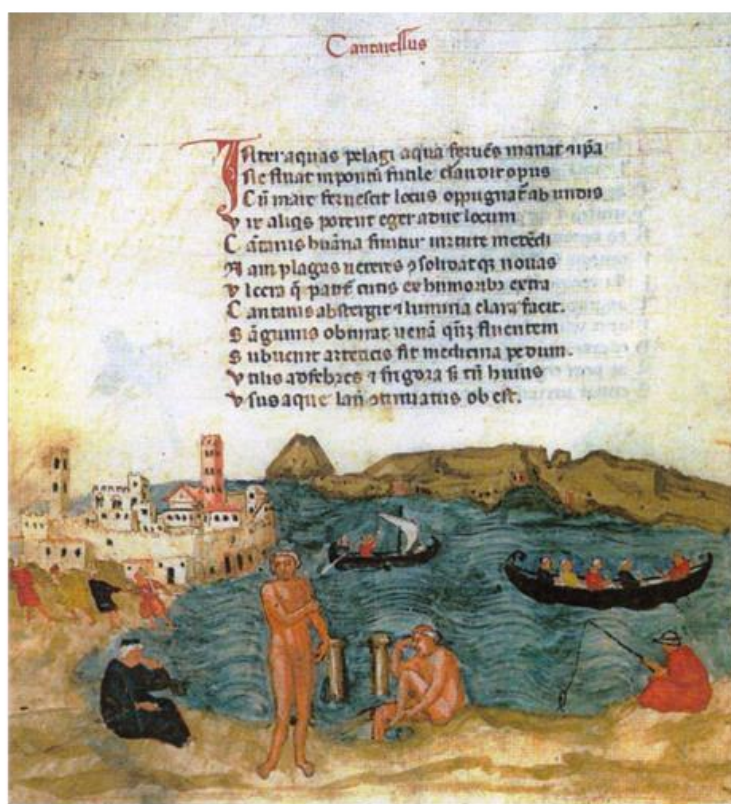


256 **Caligolian pier and to the 4th floor of Serapeum, the latter lasted until 1430. The rapid ascension**
257 **phase is also shown, associated with earthquakes of greater energy that accompanied the**
258 **emergency of the 4th floor from the sea in the early 1500s, until the eruption of 1538.**

259

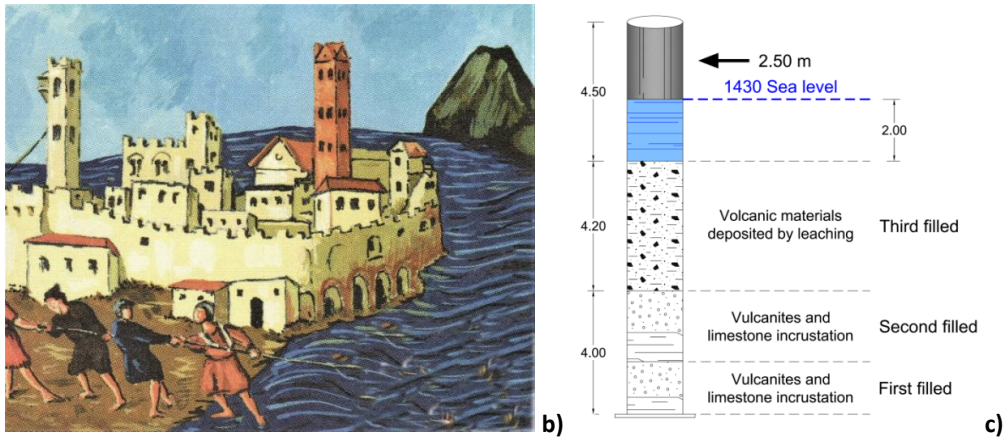
260 This observation constitutes an indication that during the time of the painting (1430), in the absence
261 of 1538 products, the buried part of the columns should then have been approximately 8 meters.
262 Moreover, the presence of trawling fishermen in the scene (Fig. 7b) suggests that sea depth there did
263 not exceed 2 m (the maximum water depth for this type of fishing not far from the beach). Given that
264 the total height of the columns is 12.7 m, we estimate that the emerged part of the column in 1430
265 was around 2.0-3.0 m (Fig. 7a,c).

266



267

a)

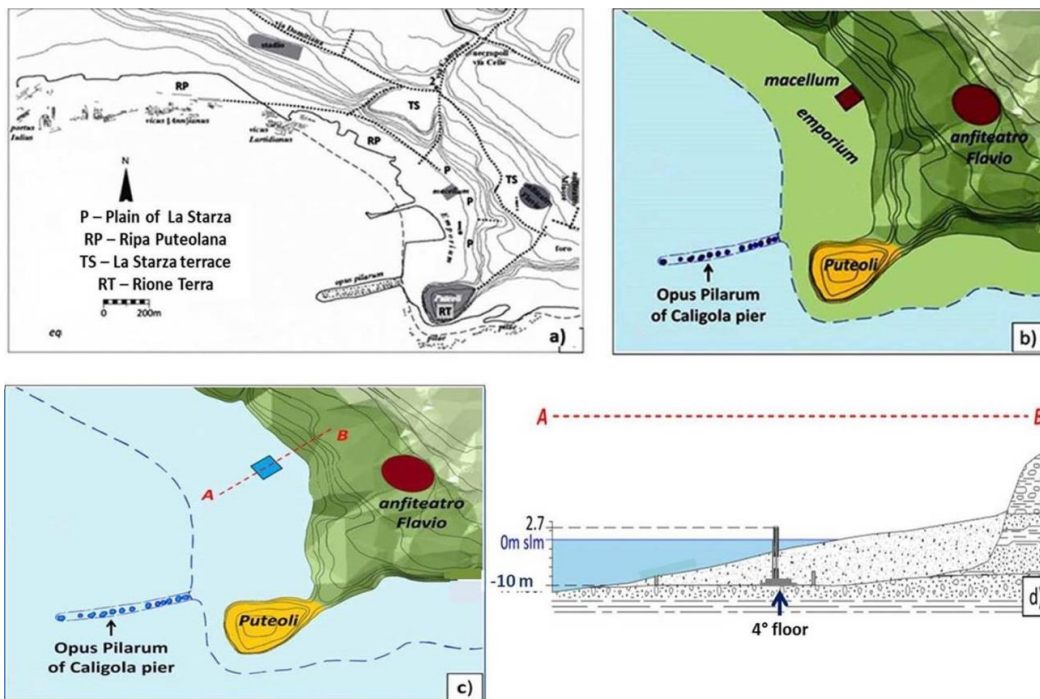


268

269

270 **Fig. 7 – Gouache de de' Balneis Puteolanum from 1430: a) Stumps of the Serapeum columns**
271 **that protrude from the sea to a height of 2-3m, b) Fishing from the shore, highlighted in the**
272 **box, indicates a draft depth of approximately 2m of sea, c) Since the columns are 12.70m high,**
273 **it can be deduced that the remaining part of the columns wrapped in the underlying sediments**
274 **is approximately 8m. From the figure it can therefore be deduced that the 4th floor of the**
275 **Serapeum in 1430 was 10m below sea level**

276



277



278 Consequently, we infer that in 1430 AD the floor was about 10 m (+/-1 m) below sea level (Fig. 6).
279 Such deduction derived from the context represented in Fig.7a, can be explained in even greater detail
280 with the help of the topographic map of the Pozzuoli area in Roman times (Soricelli 2007)
281 (Fig. 8a).

282

283 **Fig. 8 – a) Map from the Roman era (Soricelli 2007), with our own reworking, based on the**
284 **indications of Aucelli et al. (2020) and Taravera (2021). The map shows the lower part of the**
285 **emporium which extends along the Puteolana bank (RP), until reaching the base of the hill, the**
286 **so-called Starza plain (P) and the upper part of the Rione Terra cliff (RT) which, in turn,**
287 **connects with the upper hilly part of the Starza terraced area (TS), b) Part of the previous map**
288 **limited to the Emporium Area, c) the area b subject to the subsidence phase which ended in**
289 **1430, during which the hill areas (TS, RT) were surrounded at the base by the sea, according**
290 **to a description of the lower area of Pozzuoli from 1441 "the sea covered the littoral plain, today**
291 **called Starza" (De Jorio, 1820; Dvorak and Mastrolorenzo, 1991), d) note that in the profile A-**
292 **B the sea extended behind the Serapeum on the plain of La Starza hill, intersecting the columns**
293 **at a height of 10m (also shown).**

294

295 The map (contour lines of 5m), shows that in the period of greatest development, the city included
296 the Greek Acropolis (the ancient Dicearchia nowadays called Rione Terra), with a maximum height
297 of 40 m asl, the lower part of the city, i.e. the western area overlooking the ancient emporium and the
298 Serapeum (Roman macellum) placed near the bay area and the upper city, on the Starza terrace, with
299 elevation between 30-50 m asl. The latter was the site of the ancient monumental edifices
300 (amphitheatre, stadium, forum, necropolis, etc.). From this map, considering only the area of the
301 Emporium (lower part) and amphitheater (upper part), a sketch of topographical relief above the sea
302 level (in Roman times, Fig. 8b) and underlying sea level (in 1430 AD, Fig. 8c) has been obtained and
303 described as follows:

304 - from profile A-B of Fig. 8c, as reported in Fig. 8d, it can be seen that the 4th floor of the Serapeum
305 is located at a depth of 10m, packed in the sediments that form the Ripa Puteolana (RP), with the
306 columns protruding from the same sediments for 4.5m, of which approximately 2m are sea water. It
307 is indicated, ultimately, that the sea level intersects the columns of the Serapeum at a height of
308 approximately 10 m, connecting with the contour line of 10 m, on the La Starza Plain (P) (Fig. 8c,d).

309 - Fig. 8c also allows us to highlight the morphological conditions of the Rione Terra, which, as we
310 have already observed, has been described by the chroniclers who visited this place from the 11th to



311 the 13th century as "an unapproachable mountain completely surrounded by the sea" (see Jamsilla
312 and Fuiano, 1951 and Varriale, 2004, in supplementary historical material).

313 The historical data presented here are not in agreement with some results that appeared in a recent
314 work (Di Vito et al 2016), based on the following considerations:

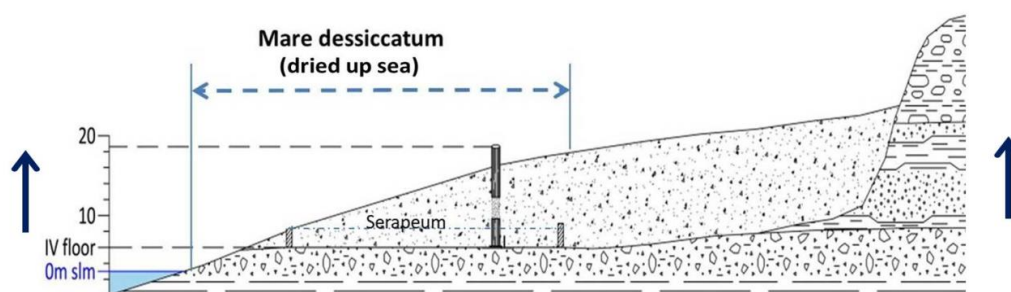
- 315 1) the subsidence in the area started in 35 BC;
- 316 2) the local uplift in the area of the 1538 vent, from 1536 to 1538, amounted to about 19 m.;
- 317 3) the maximum subsidence was reached in 1251.

318 The first claim is in contrast with at least two strong evidences, coming from historical documents:
319 the first one, that already at the times of Greek colonization (end of 8th century BC) the Via Herculea
320 used by Greeks, showed signs of subsidence (see Diodoro Siculo in Appendix 1) (Fig. 2). Limiting
321 ourselves to the 1st century BC, it is sufficient to observe that since 60 BC, due to the subsidence of
322 this dam, Giulio Cesare himself was sent by the Roman Senate in 58 BC, to fix the problem, which
323 was resolved more constructively by Agrippa in 37 BC, raising the surface of the Via Herculea with
324 respect to the sea level (see again detailed explanation in Appendix 1).

325 Claim 2) can be easily demonstrated to be not realistic, because in case of uplift in the Monte Nuovo
326 area higher than few meters, the Via Herculea would have risen back above the sea level (Fig.3d).

327 Claim 3), finally, is not confirmed by the testimonies collected until 1430, which instead indicate the
328 continuation of this phenomenon (Di Bonito and Giamminelli, 1992; Bellucci et al., 2006).

329



330

331 **Fig. 9 – The uprise of the land (marked by the two arrows on the sides) was observed and**
332 **described by Loffredo Ferrante in 1530: "the sea was very close to the plain which was at the foot**
333 **of the Starza hill". In this context, the 4th floor of the Serapeum had reached a height of**
334 **approximately 4 m above sea level.**

335

336 From our reconstruction, based on reliable historical documentation, we demonstrate that the
337 hypothesis that maximum submergence depth of the 4th floor of the Serapeum was reached in the 9-
338 10th century, proposed by Parascandola (1947) and Amato and Gialanella (2013), is not realistic. Nor



339 it is the hypothesis by Di Vito et al. (2016), who place the date of the transition between subsidence
340 and uplift in the 13th century and precisely in 1251.

341 Let us remember that, as observed in recent unrests, uplift at Campi Flegrei area, which will be
342 described well later, is accompanied by seismicity (Dvorak and Gasparini, 1991; Kilburn et al., 2017;
343 Troise et al., 2019). For many centuries, after the 9th century, and for two centuries, after the 13th
344 one, there is absence of historical evidence for significant seismicity. In the period since 1430 to 1580,
345 on the contrary, there is abundance of chronicles describing significant seismicity, how will be
346 detailed later in this work (see Fig. 19a). Our findings dating the starting phase of uplift around 1430
347 is also supported by the documented occurrence of a powerful earthquake in 1448 (Colletta, 1988:
348 see also next paragraph), which induced King Ferdinand I of Aragon to suspend the so-called
349 "fuocatico" (a mediaeval tax collected for each fire lit by a family unit). It is also well known that,
350 between 1503 and 1511, the municipality of Pozzuoli granted the lands that emerged, as a result of
351 the increasingly "drying up sea" (Fig. 9), expanding the available land, to citizens requesting them
352 (Parascandola, 1947). The next important question is then: was the 4th floor of the Serapeum above
353 sea level as early as at the beginning of 16th century? Parascandola (1947) answered this question
354 through a sentence found in an account by Loffredo Ferrante from 1580: *In 1530 the sea was very*
355 *close to the plain which was at the foot of the Starza hill* (Fig. 8). So, it can be deduced that the floor
356 of the Serapeum in the 1503 was just above sea level, that is, it had risen about 10m in about 73 years,
357 with a minimum rate of 160 mm/y. There is clear evidence that the uplift phase continued until 1538,
358 when the eruption occurred, whereas seismicity continued for the next 40 years, until 1580 (we
359 postpone the discussion of this topic to the next section). The maximum uplift occurred in the
360 Pozzuoli area, close to the Rione Terra cliff, that up to the 1538 eruption reached an elevation in the
361 order of 5-6 m asl (Fig. 6).

362 In the nearby area facing Averno to the west, the uplift, as already said, was unable to cause emersion
363 of the Via Herculea, and only a small area including the vent was affected by an uplift of about 7m,
364 i.e. slightly higher than the uplift at Pozzuoli. In the eastern sector of the caldera, at Nisida island, the
365 pier did not emerge above sea level (Parascandola 1947). It is then very likely that the uplift phase
366 had a bell-shaped trend, very similar to what we see in the recent unrests, with the sole anomaly of
367 the sharp pre-eruptive uplift of Monte Nuovo, likely due to the upward migration of the dyke feeding
368 the eruption.

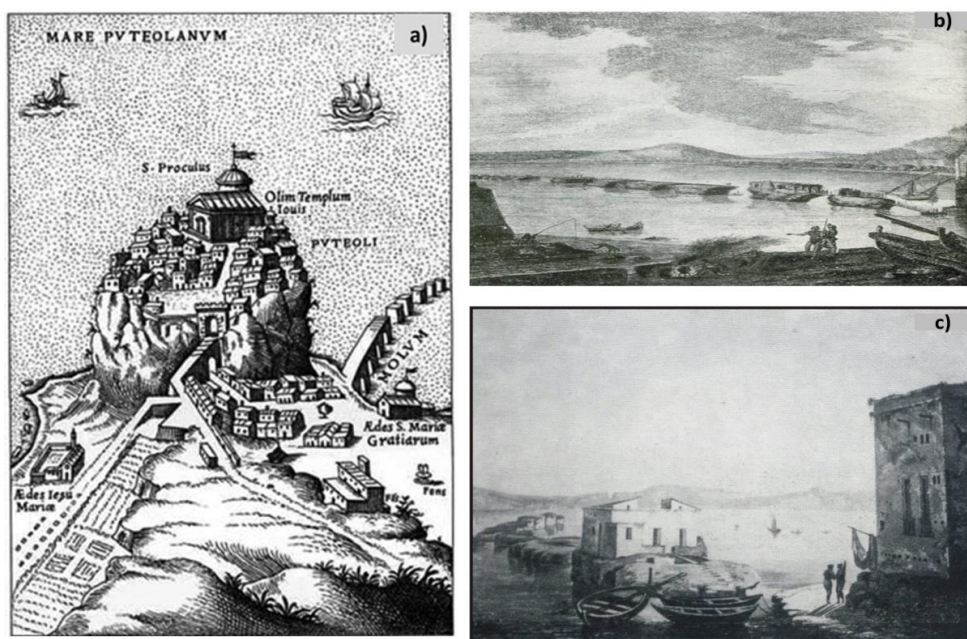
369

370 4. Ground movements after the 1538 eruption

371 The period between the end of the 16th century and the beginning of the 17th century lacks any written
372 historical document testifying the ground movements at Pozzuoli. It is likely that after the 1538



373 eruption a subsidence phase started. We can anyway learn something from some paintings, the oldest
374 one by Cartaro, dated 1584 (Fig. 10a), which highlights the Rione Terra in the foreground, with the
375 Neronian pier which emerges almost completely above sea level, which means for about 5-6 m.



376
377 **Fig. 10 – a) Engraving by Cartaro (1584) showing the Neronian pier at the base of the Rione**
378 **Terra, emerging from the sea for 5-6m, showing 10 of the 15 piles of which it was made up in**
379 **roman epoch, b) The remains of the pier piles, without the upper arches, highlighted in an**
380 **engraving from the mid-18th century, c) Detail of the same piles highlighted in another**
381 **engraving from the same period, where the height of the 1-2m piles is observed in more detail,**
382 **subject to marked erosion**

383

384 It also appears still partially complete, with about half pylons still connected with arches (*Opus*
385 *Pilarum*). In comparison, paintings from the middle XVIII century (Fig. 10b,c) report the pier
386 completely destroyed, and clearly almost completely submerged; the painting of Fig. 10c represents
387 the pylons in more detail, allowing to estimate the height of the emerging part asl around 1-2 m. Fig.
388 11 shows another famous painting of 1776, by Hamilton, which shows the ruins of the Neronian pier
389 almost the same way than in Fig. 10b,c and, in addition, shows the columns of Serapis Temple, with
390 its floor almost at the same level than the Neronian pier.

391



392

393 **Fig. 11 – a) View of the Gulf of Pozzuoli and the Cape Miseno peninsula (Hamilton 1776).**

394 **Both the remains of the Neronian pier and the newly excavated Serapeo are also visible**

395



396

397 **Fig. 12 – Serapeo excavated in the three-year period 1750-1753. It can be noted that the height**
398 **of the lighter parts of the columns, including the pitted band of the lithodomes, is preserved by**
399 **oxidation, because packed by the newly removed sediments. The darker upper part, oxidized**
400 **since staying outside the cover, has a height of approximately 2.50m, estimated on the same**
401 **figure. This leads us to consider that the band of sediments removed had a thickness of**
402 **approximately 10m, that is, the height of the hill where the *vineyard of the three columns* was**
403 **located before the excavation (Niccolini, 1842).**



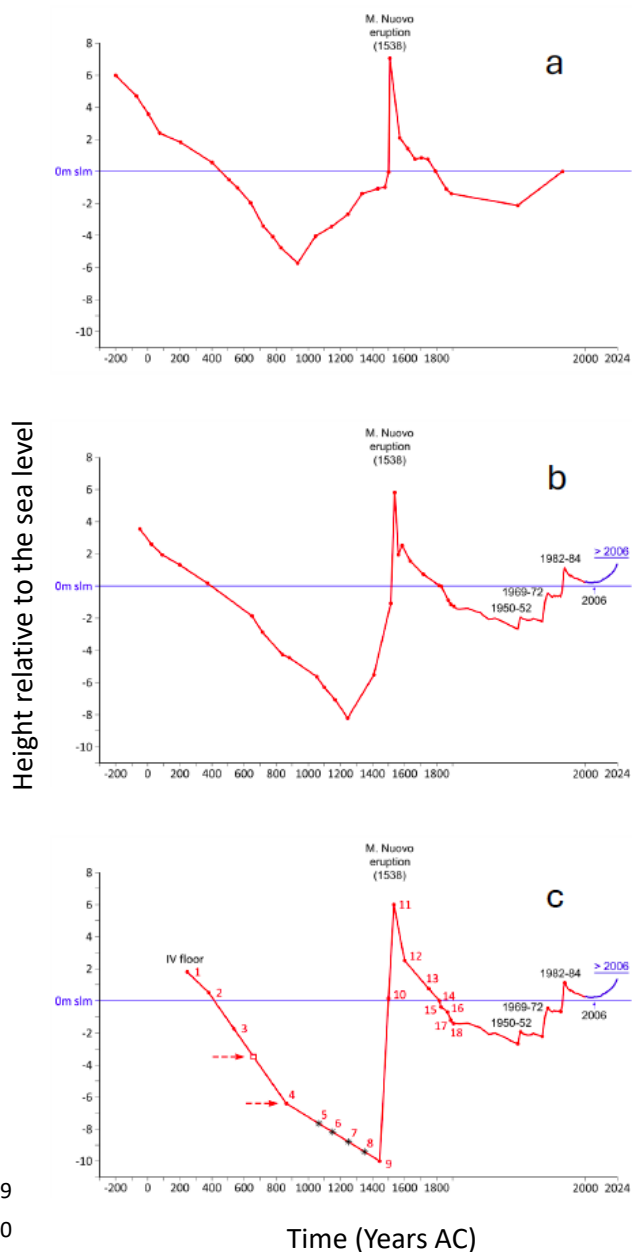
404

405 From the comparison between Fig. 10a and 10b, c it can be deduced that the Roman opus pilarium
406 underwent a subsidence of about 4-5 m. from 1580 to 1750.

407 Since the floor of the Serapis Temple appears to be at the same level than the pier, its level in 1538
408 can be estimated as 5 – 6 m. above sea level (Fig. 6), while in 1750 it should be at about 1m above sea
409 level, with an estimated subsidence 1580-1750 of about 4-5 m. This approximate estimation is however
410 confirmed by Parascandola (1947), who reports some measurements by Niccolini (1846), who found
411 the 4th floor of Serapeo to have a height above sea level varying in the range 0.9 - 0.6m throughout
412 the 18th century. It can then be deduced that during the three years of the excavations (Fig. 12) the
413 floor could have been approximately at 0.7 m above sea level.

414 Finally, we want to highlight, in agreement with Parascandola (1947), that the subsidence of 4 - 5 m,
415 started after 1538-1580, could have evolved at higher initial rate, in such a way that, around the middle
416 of the 17th century, it already had a value of 2 -3 m, and then slowed down towards the end of the
417 century, until the 1750.

418 We are hence able to describe in more detail the whole evolution of ground movements at the Pozzuoli
419 area since Roman times, including the period following the 1538 eruption and until today. Such a
420 reconstruction is shown in Fig. 13c. In particular, regarding the post-1538 subsidence phase, the data
421 shown, starting from the 17th century, have been combined with those obtained by the most
422 significant measurements carried out by numerous researchers who dealt with this phenomenon
423 during the 1800s, as reported by Parascandola (1947), who suggested the reconstruction shown in
424 Fig. 13a. High precision, frequent measurements started to be collected since 1905, initially based on
425 leveling survey carried out by the Military Geographic Institute (IGM). Data from the levelling
426 surveys were still provided also during the occurrence of the most recent unrest phases, i.e. in 1950 -
427 52, 1969 – 72, 1982 – 84 and until 2001. Since 2001, continuous measurements are provided by GPS
428 (RITE, see Fig. 13b,c) installed at Rione Terra (Del Gaudio et al 2010).



429
430
431

432 **Fig. 13 a) Reconstruction of the ground level of the Serapeum floor, with respect to the mean**
433 **sea level (blue line), as proposed by Parascandola (1947); b) The reconstruction of the Serapeum**
434 **floor ground level, since the III century A.D. to present, recently proposed by Di Vito et al.**
435 **(2016); since the III century A.C. to today; c) The reconstruction of the ground level of the**
436 **Serapeum IV floor, since III century A.D. to present, inferred by this study. Each point in the**



437 **diagram corresponds to an appropriate historical indication reported in the text and/or in the**
438 **appendix.**

439

440 **5. Schematic model for the preparatory phases of the 1538 eruption**

441

442 **5.1 Dynamics of the resurgent block in response to temperature and pressure** 443 **perturbations**

444 The ground deformation at Campi Flegrei, during the phases preceding and following the 1538
445 eruption, has been likely very concentrated in a small area of few km of radius around Pozzuoli, just
446 as during the recent unrests (De Natale et al., 2001; 2006; 2019). Such a concentration is in agreement
447 with the presence of a resurgent block.

448 Evidence for the involvement in the Campi Flegrei unrest episodes of a resurgent block comes from
449 the first observations and modeling by De Natale and Pingue (1993). These authors pointed out that
450 the concentration of the uplift in a small area, the high uplift values, and the invariance of the uplift
451 and subsidence shape, as well as of the maximum seismic area, indicated the up and down movement
452 of a resurgent block, bordered by ring faults focusing the occurrence of earthquakes (see also De
453 Natale et al., 1997; Beauducel et al., 2004; Troise et al., 2003; Folch and Gottsmann, 2006). In recent
454 times, new evidence has been collected about the location and limits of the resurgent block (Rolandi
455 et al. 2020b). Active high-resolution reflection seismic surveys have pointed out and imaged the
456 presence, in the Gulf of Pozzuoli, of an inner resurgent antiformal structure or “block” bounded by a
457 1-2 km wide inward-dipping ring fault system associated with the caldera border, whose limits have
458 been also documented by the survey (Sacchi et al., 2014 Steinmann et al, 2016; Sacchi et al., 2020a).
459 Further constraints for the extent on-land of the resurgent block come from stratigraphic evidence. In
460 particular, the old well CF-23, drilled in the Agnano area, presents about 900 m of NYT pyroclastic
461 deposits, topped by only 100 m of more recent deposits (Rolandi et al. 2020b). The presence of
462 uplifted, thick layers of NYT, characterizes the stratigraphy of all the wells contained in the resurgent
463 block (Fig.14a,b,e), thus allowing to map its extent on-land, although only the CF-23, by far the
464 deepest one, clarifies the whole thickness of the NYT deposits in the resurgent area (Fig. 14a,c,d).

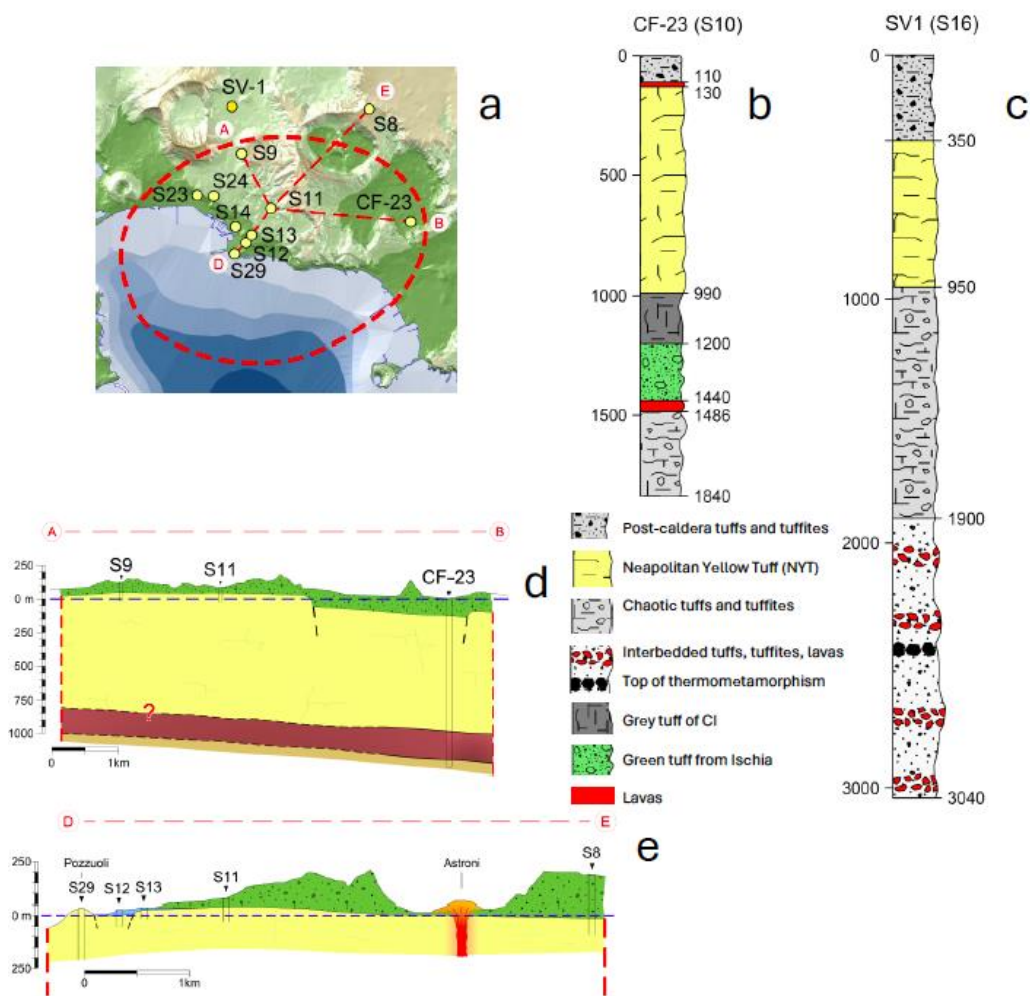
465 The extent of the resurgent block on-land appears also reasonably well defined by a clear relative
466 gravimetric maximum (Capuano et al., 2013). It is crucial to emphasize that the differential movement
467 of the resurgent block, mostly detached from the external caldera rocks, is responsible for the almost
468 constant, highly concentrated shape of ground displacement, during both uplift and subsidence. The
469 resurgent structure is also associated with distinct seismicity along the bordering ring fault zone (see



470 also Troise et al., 2003). Fig. 15a-c shows how the resurgent block is well evidenced by passive
471 seismic data (Fig. 15b, c) and by earthquake locations (Fig. 15a).

472 The presence of the central, resurgent block significantly influences the dynamical behaviour in
473 response to temperature and pressure perturbations. This is particularly evident in the central, most
474 uplifted and seismic area, where the shallow crust comprises approximately 1.5 km of tuff. This
475 contradicts substructure models proposed by various authors (Rosi and Sbrana, 1987; Vanorio et al.,
476 2002; Lima et al., 2021; Kilburn et al., 2023), which often assume a thick shallow layer of loose
477 pyroclastics from recent eruptions, typically represented by the stratigraphy of well SV1 (see Fig.
478 14e).

479 The physical state of the shallow structure within the resurgent block can be inferred by seismic
480 tomography analyses presented by several authors (e.g. Aster and Mayer, 1998; Vanorio et al., 2005;
481 Vinciguerra et al., 2006; Battaglia et al., 2008; Calò and Tramelli, 2018). These analyses consistently
482 indicate a high V_p/V_s ratio centered below Pozzuoli town down to 1-2 km, interpreted as highly water
483 saturated tuff.



484

485 **Fig. 14 - a) Location of the wells explored within the resurgent tuff block, as reported in**
 486 **literature; b) Stratigraphy of the CF23 (S10) well, within the resurgent block; c) Stratigraphy**
 487 **of the SV-1 well, outside the resurgent block, which highlights a stratigraphy where the NYT**
 488 **tuff blocks are not present with significant thicknesses; d-e) Profiles in the resurgent block**
 489 **which highlight the shallow depth of NYT because of the resurgence.**

490

491 Of particular significance is the work by Vinciguerra et al. (2006) which compared the results of
 492 seismic tomography with laboratory tests. They demonstrated that the tuffs present in the central area
 493 of the Campi Flegrei caldera can be either water or gas saturated, and that inelastic pore collapse and
 494 cracking produced by mechanical and thermal stress can significantly alter the velocity properties of
 495 Campi Flegrei tuffs at depth. The effect on velocities becomes significant when the temperature rises

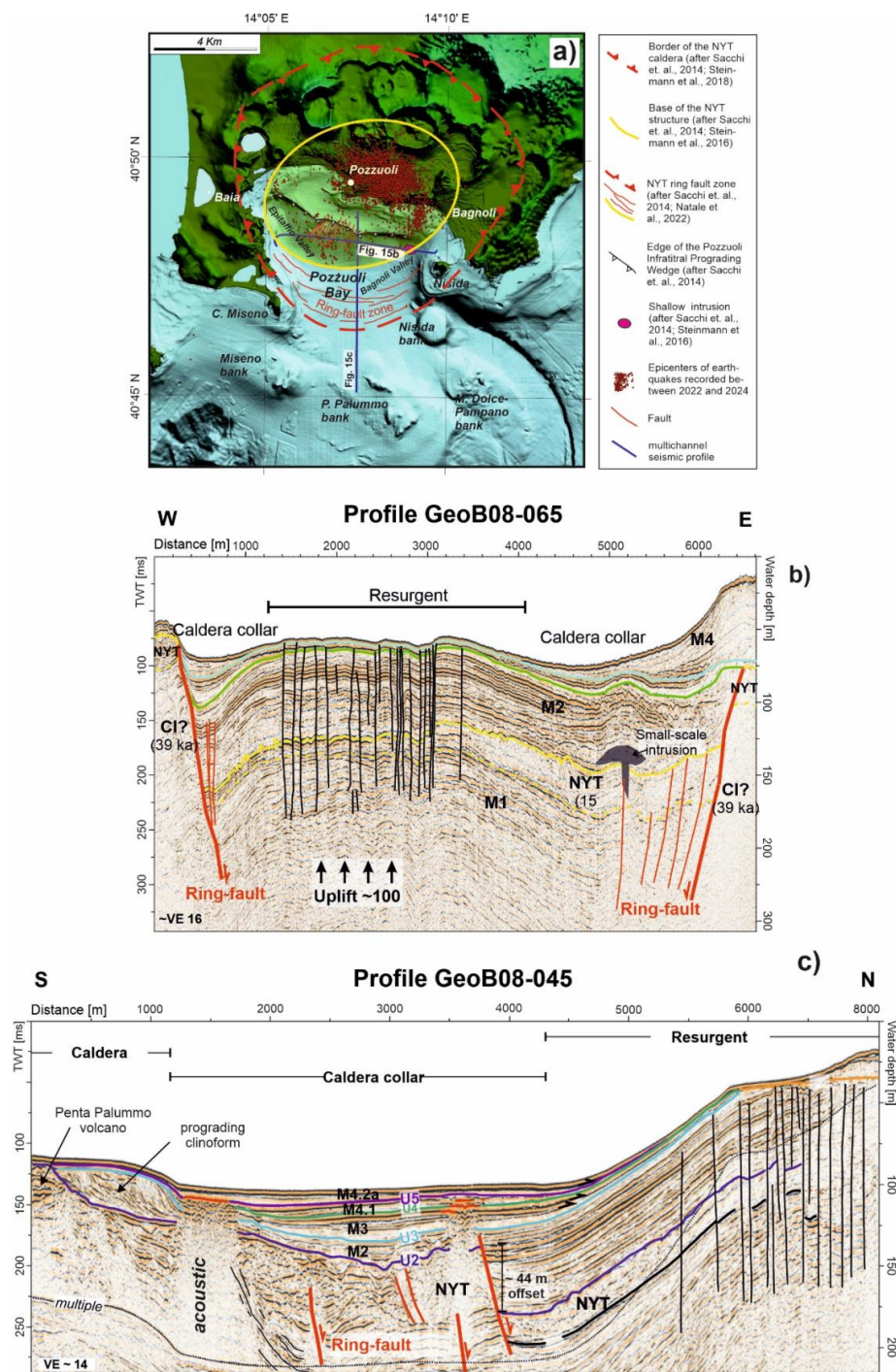


496 sufficiently to induce physical changes, such as volume change and the generation of free water
497 associated with the dehydration of zeolite phases. This can lead to thermal crack damage, further
498 influencing the dynamic behavior of the area. At higher depths, well CF-23 indicates the presence of
499 pyroclastic deposits from a depth of approximately 1.5 km to at least 1.8 km, where a temperature of
500 300°C was measured (Fig. 14b). Likely, at even greater depths of about 3km, marine silt and clay
501 layers induce silica mineralization and the formation of low-permeability horizons. Due to the high
502 temperatures, estimated to be at least 400°C, these layers undergo thermal alteration, forming a
503 thermo-metamorphosed layer (Fournier, 1999; Lima et al., 2021; Cannatelli et al., 2020).

504 Is important to note that Battaglia et al. (2008) interpreted a low V_p/V_s body, extending to about 3–
505 4 km of depth, as due to the presence of fractured overpressured gas-bearing formations, confirming
506 the data of Vanorio et al. (2005). This depth range of 3-4 km likely represents a primary accumulation
507 zone

508

509



510

511 **Fig. 15 – a)** Campi Flegrei map showing the limits of the resurgent block, which concentrates
 512 ground deformation and seismicity. The thinner black line indicates the ring fault marking the
 513 limit of the resurgent block at sea, and the thicker one the ring fault associated to the offshore



514 **caldera border. b) The N-S and c) W-E profiles of the high-resolution seismic survey, showing**
515 **the offshore signature of the NYT ring fault system and resurgent structure (from Sacchi et al.,**
516 **2014, 2020a, 2020b; Steinmann et al., 2016).**

517

518 for shallow intruded magma, which is unable to reach the surface and instead forms magma sills
519 (Woo and Kilburn, 2010; Di Vito et al., 2016; Troise et al., 2019; Kilburn et al., 2023). The magma
520 at this depth is likely to be a mush state, solidified, but still at temperature high enough to be
521 remobilized by the inflow of new magma or hot magmatic fluids (De Natale et al., 2004).

522 At even greater depths, approximately between 7 - 8 km, the main magma chamber is located. This
523 chamber contains both liquid magma and residual mush from past eruptions (Judenherc and Zollo,
524 2004).

525

526 **5.2 The preparatory phases of the 1538 eruption**

527 A tentative model can be now constructed for the preparatory phases of the 1538 eruption, which
528 accounts for all available data. It is shown in Fig. 16, and can be summarized as follows:

529 the Pozzuoli area experienced a long period of subsidence, beginning at the end of the second phase
530 of post-caldera volcanism (3.7 ka B.P.) and lasting until 1430 AD. This subsidence was likely triggered
531 by the collapse of the upper and middle crustal blocks into the underlying magma chamber, situated
532 deep within the limestone basement at depths of 7-8 km (Judenherc and Zollo, 2004). The viscoelastic
533 behaviour of the shell encasing the magma chamber may have also contributed to the subsidence, along
534 with the decrease in magma volume due to cooling and crystallization (Fig. 16a).

535 Since the end of the second phase of post-caldera volcanism, approximately 3.7 ky ago, the primary
536 magma chamber, located at 7-8 km of depth, likely contains a mixture of liquid magma and mush. It's
537 important to note that mush refers to a non-eruptible phase of trachytic magma, composed of 25%–
538 55% volume by crystals (Marsh, 1996; Bachmann and Huber, 2016; Cashman et al., 2017; Edmonds
539 et al., 2019). When heated by several tens of degrees, typically through the injection of hotter magma,
540 mush can revert to a liquid state, thereby regaining the ability to trigger a volcanic eruption (e.g. De
541 Natale et al., 2004; Caricchi et al., 2014). However, the way the mush is rejuvenated by intrusion plays
542 a fundamental role in this mechanism (Parmigiani et al., 2014). One plausible scenario is that the new
543 magma from the deeper crustal levels forms sills at the base of the mush, revitalizing it through the
544 supply of heat, but not of magmatic mass, i.e. only exsolution occurs (Bachmann and Bergantz, 2006;
545 Bergantz, 1989; Burgisser and Bergantz, 2011; Huber et al., 2011; Bachmann and Huber, 2016;
546 Cashman et al., 2017; Carrara et al., 2020). To explain the rapid uplift observed in the interval between
547 1430 and 1538, the temperature contrast between the two layers could play a fundamental role: the



548 mafic melt positioned at the base, being hotter than the overlaying layer, undergoes cooling and
549 crystallization, leading to an increase in the volatile content (primarily H₂O and CO₂) of the residual
550 melt (Fig. 16b). Lower ductile rocks tend to deform gradually, allowing magmatic gases to permeate
551 into the brittle zone above, thereby inducing a thermo-metamorphic separation layer.

552 The presence of supercritical fluids, within this zone is indicated by a seismic anomaly displaying
553 low V_p/V_s at approximately 4 km depth (Battaglia et al., 2008). Above this depth the earthquakes are
554 concentrated, suggesting the occurrence of fractured formations rich in overpressured gas. This
555 condition likely results in triggering additional earthquakes (Fig. 16a). A similar condition has been
556 often hypothesized to occur in the Yellowstone volcano (Shelly and Hurwitz, 2022). Intense degassing
557 from the main magma chamber would lead to increased pressure in the shallow aquifers. Moreover,
558 the rise in temperature would cause the water contained in the tuffs' zeolites to convert into steam,
559 generating additional overpressure. Such a situation is shown by the CF-23 well, where its
560 stratigraphy indicates the presence of a lava layer approximately 30 m thick beneath the overlying
561 tuff blocks, which are approximately 1.5 km thick (Fig. 14b).

562 It is noteworthy, when considering the correct stratigraphy of the resurgent block, as represented by
563 the CF-23 well, that some previous models suggesting the presence of two low-permeability layers
564 at depth (Vanorio and Kanitpanyacharoen, 2015; Kilburn et al., 2023), inferred from the SV1 well
565 (which is situated outside of the resurgent block) (Fig. 14a), appear to be incorrect. Therefore, above
566 the thermo-metamorphic zone, magmatic gases do not accumulate below the hypothetical second
567 low-permeability layer, as postulated by Kilburn et al. (2023), but rather between the summit lava
568 base and the underlying thermo-metamorphic horizon, corresponding to a depth of 2.5 km, which is
569 the fragile layer. Consequently, at the base of the lava body, conditions of high temperature and
570 pressure result in widespread brittle deformation of this layer due to uplift, rendering it highly
571 permeable by fracturing (Fig. 16b).

572 Finally, super-compressed magmatic gases were likely contained within approximately a 2.5 km thick
573 fragile zone, while a limited release of the increased pressure occurred directly through the fractures
574 connecting the intermediate depth area with the Solfatara and Pisciarelli areas, resulting in the escape
575 of CO₂-rich vapor, as evidenced by the reported increase in fumarolic activity (Chiodini et al. 2021).
576 Following this hypothesis, it is noteworthy that, at a depth of 1.8 km, the CF23 drill-hole indicates a
577 very high temperature of 300°C, not far from the supercritical temperature. It is plausible that, if the
578 temperature significantly increases, due to the supply of deeper, hot magmatic fluids, the water
579 contained in the basal part of the tuff block could reach supercritical conditions, leading to thermal
580 fracturing within the tuff block (Vinciguerra et al., 2006), over a certain thickness (Fig. 16b).



581 As previously mentioned, the increase of pressure resulting from such intense heating caused by deeper
582 magmatic fluids should be attributed to both the overpressure of shallow aquifers and the vaporization,
583 of water contained in the zeolites, likely in the form of superheated steam.

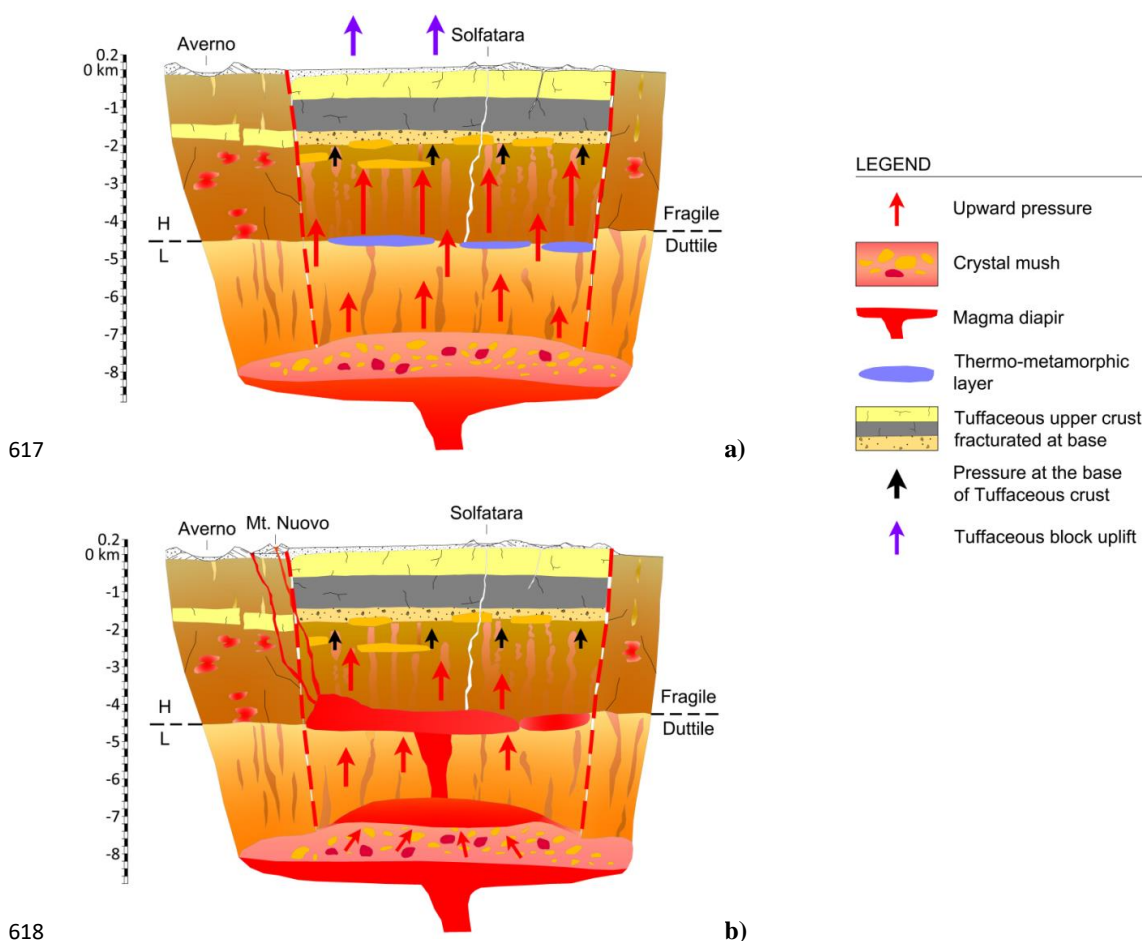
584 In conclusion, the uplift in the Pozzuoli area cannot be attributed solely to magmatic fluids
585 pressurizing the layer above the thermo-metamorphic horizon (Nespoli et al., 2023; Kilburn et al.,
586 2023), nor solely to the increase of pore pressure in the shallow aquifers (Casertano et al., 1975; De
587 Natale et al., 1991; Scafetta and Mazzarella, 2021). Our hypothesis includes the presence of various
588 sources originating at different depths, collectively contributing to the uplift dynamics underlying the
589 area of maximum uplift during the period from 1430 to 1503 and coinciding with the phase we
590 designate as the 'long-term seismic precursors' (see next section). These sources include
591 approximately 2.5 km of brittle crust enriched in gases under supercritical conditions, along with
592 overheated conditions in the upper part. Together, these factors act as the driving force behind the
593 uplift observed in the region during this specific period.

594 The pressure increases in the main magma chamber, resulting from the input of new magma and/or
595 magmatic fluids, can trigger the formation of magma sills (Troise et al., 2019). The progressive
596 intrusion of several magma sills likely leads to the ascent of magma towards the surface. This process
597 may be further facilitated by phreatic explosions caused by the heating of shallow aquifers, resulting
598 in depressurization pulses. Intruding magma may encounter layers that are more resistant to
599 penetration at certain depths. In this case further magma intrusion may be inhibited and lateral
600 expansion, to form sills, may occur (Gretener, 1969). Previous studies of recent unrests have indicated
601 that depths between 2.5 and 4 km, close to the upper limit of the ductile zone, are locations where
602 magma intrusions can halt (Woo and Kilburn, 2010; Troise et al., 2019). Before the 1538 eruption, a
603 small plumbing system, in the form of flattened intrusions near the contact between a lower ductile
604 zone and an upper brittle zone in a high-pressure environment, was hypothesized (Fig. 16b) (Pasquare
605 et al., 1988). From such a shallower magma chamber, magma can further progress upward towards
606 the surface. A dynamic in which early intrusions in the shallow crust create small plumbing systems
607 (i.e. stalled intrusions), from which a dyke later propagates, bringing a small quantity of magma to
608 the surface, is typical of monogenic volcanoes (Marti et al., 2016). The ability of intruded magma
609 sills to erupt at surface is also influenced by the relatively short timescale of sill solidification,
610 typically in the order of ten to twenty years (Troise et al., 2019).

611 Shallow solidified magma sills, in the form of mush, can be remobilized due to the arrival of new
612 magma and/or the introduction of hot deeper magma fluids. The significant uplift preceding the 1538
613 eruption, amounting to more than 16 meters in the initial phase involving the entire resurgent block,



614 could be interpreted solely in terms of magma intrusion suggesting a total intruded volume, in the
 615 shallow plumbing system, on the order of a cubic kilometer of magma, at least (Bellucci et al., 2006).
 616



620 **Fig. 16 – Schematic cross sections of the hydrothermal and magmatic systems underlying the**
 621 **Campi Flegrei resurgent block in the 1538 AD, showing:**

622 **a) Process of gas sparging according to Bachmann and Bergantz (2006) model, related to the**
 623 **transfer of hot gas from a mafic intrusion underplating the trachytic mush and the hypothesized**
 624 **relation with earthquake swarms of the exsolved fluids, accumulated at lithostatic pressures in**
 625 **the ductile region and episodically injected into the brittle crust at very high strain rates. The**
 626 **sudden increase of fluid pressure, in the brittle region, triggers earthquake swarms in the 2-4**
 627 **km depth range.**



628 **b) Remobilization of mush by mafic magmas then occurs, so that the magma remobilized from**
629 **the mush accumulates at the top, fueling its rise upward to accumulate, in a sill-like shape, along**
630 **the ductile-brittle transition surface. Eruption from the magma sill is then likely to occur at the**
631 **faulted borders of the resurgent block.**

632

633 However, despite such a large volume of shallow intruded magma, the eruption of 1538 only
634 produced about 0.03 km³ of pyroclastic deposits (see next section). This discrepancy likely suggests
635 that multiple sill intrusions occurred over more than one century, with most of them solidifying
636 without contributing to the eventual eruption. Only the most recent intrusion events, and/or some
637 portion of magma mush from prior intrusions remobilized by subsequent heating, would have fed the
638 eruption.

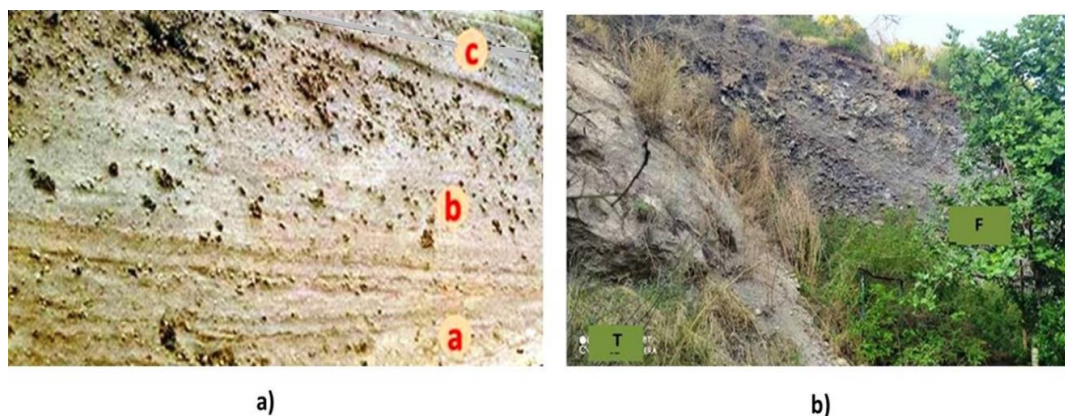
639 Another characteristic of eruptions from small monogenic volcanoes is their difficulty to forecast, as
640 they occur at unexpected locations (Marti et al., 2016). Both distinctive traits were evident in the
641 eruption of Monte Nuovo, which represents a prototype of a small monogenic volcano in the Campi
642 Flegrei. Despite the relatively small volume of magma (0.03 km³), the eruption occurred at a
643 considerable distance, approximately three km westward, from the area of maximum uplift. The
644 position of the 1538 vent is approximately on the border of the resurgent block: such a border, marked
645 by ring faults, clearly represents a weak zone, where magma can more easily intrude.

646 **5.3 The eruption of 1538**

647 The week preceding the eruption, was marked by a series seismic events (Guidoboni and Ciuccarelli,
648 2011). The shoreline gradually retreated 200 steps (ca. 370m) seaward, because of an occasional uplift
649 occurred on the eastern shore of Lake Averno (see Fig. 2d) and during the 36 hours preceding the
650 eruption, there were 7 meters of ground uplift (Parascandola, 1943; Costa et al., 2022). The local uplift
651 rapidly attenuated as a function of distance, adding about 1-2m to the maximum uplift in Pozzuoli
652 (Rolandi et al., 1985) (Fig. 6). The uplift, involving a local marine regression, was accompanied by
653 strong rumbles on the night between 28 and 29 September, culminated in a further explosion, at 2 am
654 on the following night, which marked the vent opening and the start of the eruption. The early eruptive
655 column, initially white in colour, ejected muddy ashes and lithic and scoriaceous lapilli upwards. The
656 presence of wet ash on the slopes of the gradually growing volcanic cone led Parascandola (1943) to
657 hypothesize that it was a mud eruption. This description, present in the chronicles of the time
658 (Parascandola 1943), indicates that the first eruptive phase was phreatomagmatic in character, although
659 it evolved with a peculiar characteristic, because the volcanic cone was formed by massive pyroclastic
660 units, made up of loose and wet deposits, ascribable to pyroclastic flows products with a prevalent
661 sandy matrix, incorporating lithic and scoriaceous clasts. In Fig. 17a we recognize three main flow



662 units, each of them made up of sub-units. These sub-units are mostly evident in the finest basal part
663 (a), while in the intermediate part (b), showing abundance of scoriaceous clasts, an inverse gradation
664 is observed. Finally, the hydromagmatic activity, lasted about 12 hours, built a small tuff cone, formed
665 by successive waves of pyroclastic flow units, whose deposits reached a height of approximately 120
666 m. This particular type of hydromagmatic deposit implies an eruption in which the magma-water
667 interaction process is characterized by a low efficiency, considering the thermal energy of the magma
668 and the mechanical energy generating the eruption. In the classic Wohletz experimental diagram
669 (Wohletz et al., 2013), besides the fields 1 and 3 which include, respectively, eruptions with zero or
670



671

672 **Fig. 17 – a) Flow units in the phreatomagmatic Pyroclastic flows, b) Deposit of the final scoria**
673 **flow (F) deposited in the western depression of the phreatomagmatic Tuff cone (T).**

674

675 low magma/water ratio (0 – 0.1) and those with extremely high ratios (100-1000), field 2 includes
676 hydro-magmatic explosive eruptions with an interaction ratio between 0.1 – 10, indicative of a greater
677 value of mechanical efficiency (Fig. 18). It is evident, however, that even in field 2 there is a
678 differentiation in efficiency, due to the condition characterizing the expansion of the water vapor that
679 develops during the magma-water interaction process, that is:

680 1) If the magma/water ratio is around the value of 0.3, the maximum efficiency is achieved. The
681 quantity of water is optimal and expands entirely as superheated steam, that is, the maximum volume
682 that can be generated is obtained without dispersing heat. Under this condition, the so-called Base
683 Surges are formed;

684 2) If the water content increases, the efficiency drops because not all water is vaporized, and, as a
685 result steam saturated with water is formed. Under this condition, Pyroclastic flows are formed.

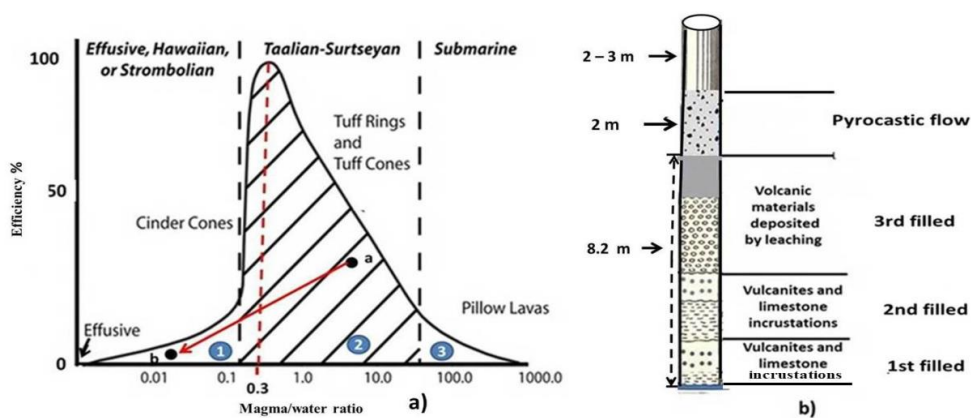


686 This last type of flow is therefore associated with the collapsing eruptive columns that developed in
 687 the night between 29 and 30 September, to be ascribed to a phreatomagmatic eruption with a high
 688 magma-water ratio, which gave rise to the non-welded ignimbrites described in typology 2 and located
 689 in the diagram of Fig.18a, at point a. This implied that in the initial phase of the eruption the magma
 690 absorbed a considerable quantity of sea water present above the eruptive vent, so in these conditions,
 691 the collapsing eruptive columns which gave rise to the pyroclastic flows on the night between the 29th
 692 and 30th September, reached a maximum height of less than 3 km, (Parascandola, 1943), depositing
 693 in a radius of approximately 3 km, as follows:

694 - with thickness of 5-10m, in sections obtained by cutting the slope in the area around the volcano (Fig.
 695 17a);

696 - in a depression on the SE sector of the volcano. The materials of the Tuff Cone of Monte Nuovo (T)
 697 are present, together with the products of the scoria flow (F) deposited in the SE depression (Fig. 17b).

698 It should be noted that, about 1km away towards the SE, in the direction of the Serapeum, the products
 699 of the Tuff Cone display a thickness of about 5m and around the Serapeum itself



700
 701 **Fig. 18 – a) Wohletz (1983) diagram for the evaluation of the mechanical efficiency of the**
 702 **products emitted in the form of Pyroclastic flows and fall/flow from Strombolian eruption**
 703 **column collapse, b) products emitted by the 1538 eruption in the first eruptive phase as wet**
 704 **pyroclastic flow, which bury the upper part of the Serapeum columns (above 8.2 m of height).**

705
 706 (about 3km away), the products show a thickness of about 2m (Fig. 18b). According to the chronicles,
 707 on October 6th there was a new eruptive phase and 24 unwary visitors died, surprised by the
 708 resumption of eruptive activity, which revealed itself with different characteristics, mainly magmatic,
 709 that is, with a low water-magma interaction ratio (point b in Fig. 18a). In the hydromagmatic-magmatic
 710 transition, the eruptive cloud took the characteristic ‘cauliflor’ shape of Strombolian eruptions, with a



711 height of about 4 km, which, driven by winds from the NW and then from the N, distributed the
712 scoriaceous products towards the SE in the direction of Nisida and the Neapolitan coast, then towards
713 the S, in the direction of Bacoli and Capo Miseno (Parascandola, 1943). The scoriaceous products of
714 the second Strombolian magmatic eruptive phase uniformly covered the basal units that formed the
715 volcanic edifice during the first phase, with an average thickness of about 0.5 m. The final phase of
716 the eruption occurred with the collapse of the Strombolian eruption column, which deposited a scoria
717 flow in a depression on the eastern side of the underlying cone of materials formed by phreatomagmatic
718 pyroclastic flow units (Fig.17b). Overall, the eruptive event of 1538, with the emission of 0.03 km³ of
719 pyroclastic material, can be classified with a VEI = 2.

720

721 **6. The seismicity before and after the 1538 eruption**

722

723 The main precursors of the eruption, as reported by chronicles, were the earthquakes. Earthquake
724 sequences preceded, accompanied and followed the 1538 event. In this context, seismic precursors
725 may depend on the occurrence of stress perturbation, determined by the arrival of magmatic gases, as
726 well as directly by magma intruded at shallow crustal levels (typically at depth of 3-4 km), originating
727 from the main reservoir located at about 7.5-8.0 km depth.

728 We analyze here the earthquake sequences that occurred before the eruption.

729

730 **6.1 Comparing past and recent earthquakes: from intensity to magnitude**

731 To better compare the past **earthquakes** with the recent and present-day seismicity recorded at Campi
732 Flegrei we must convert intensities in magnitude. In Fig. 19, we present a tentative correlation
733 between the epicentral intensity (I_0) and the magnitude (M_L). Choosing the correct relation between
734 I_0 and M_L is not straightforward, particularly in this case involving peculiar volcano-tectonic
735 earthquakes. Nonetheless, it is important to establish such a relation to compare the seismicity
736 observed during the 1430-1582 period, as inferred by Guidoboni and Cucciarelli (2011), with the
737 seismicity experienced during the recent unrests. To determine the I_0 - M_L relation, we are confident
738 that, despite the availability of several formulas in the literature, the best approach is to consider a
739 precise geographical and seismotectonic context, especially in a volcanic setting. Different features
740 allow to discriminate between volcanic and tectonic earthquakes, which suggests caution in using
741 correlations derived from tectonic areas for volcanic earthquakes, and vice versa (Milana et al., 2010).
742 In order to build a realistic relation between seismic intensity and magnitude in this area, we utilized
743 the computed intensities of two earthquakes that occurred in the Campi Flegrei region in 1983
744 (Branno et al., 1984; Marturano et al., 1988; Milana et al., 2010; Charlton et al., 2020), during the



745 previous unrest of 1982-1984 (Troise et al., 2019). Additionally, we considered a $M=5.0$ earthquake
746 that occurred in the similar volcanic area of Colli Albani (Sabetta and Paciello, 1995). The $M=4.0$
747 earthquake occurred on October 4, 1983, at Campi Flegrei, was found to have a maximum intensity
748 $I_0=VII$ (Branno et al., 1984; Marturano et al., 1988). An earthquake of magnitude $M=3.5$, which
749 occurred in the same swarm on October 4, 1983, was found to have a maximum intensity $I_0=V$ (Fig.
750 19: Marturano et al., 1988). Furthermore, Sabetta and Pugliese (1995) reported an earthquake of
751 $M=5.0$, with a maximum magnitude $I_0=VIII$.

752 These correlations between intensity and magnitude were utilized to assign realistic magnitude values
753 to the macroseismic intensities deduced from the analysis of historical seismicity (Guidoboni and
754 Cucciarelli, 2011), as shown in Fig. 19. They were also used to transform the magnitude of
755 earthquakes associated with recent unrest phases into macroseismic intensities, as we will discuss
756 later.

757

758 **6.2 The seismic phases that accompanied the ground uplift and the eruption**

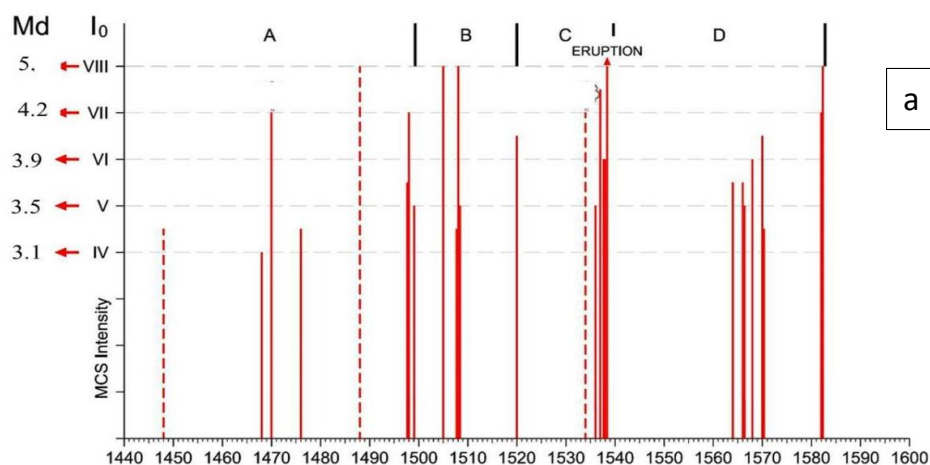
759 We can classify the precursory earthquake sequences into three categories: long-term, medium-term
760 and short-term precursors.

761 - The phase of *long-term seismic precursors*, preceded by historical reports of earthquakes of
762 doubtful occurrence, began to be well documented since 1468 - 1470, when a paroxysmal seismic
763 phase occurred ($I_0 = VII$) (Guidoboni and Ciuccarelli, 2011; Francisconi et al., 2019) (Fig. 19a –
764 interval A), resulting from a progressive increase in fracturing. This culminated into intense
765 fumarolic-hydrothermal activity recorded at the Solfatara volcano. The historical chronicles report
766 widespread damage to the vegetation, both spontaneous and cultivated, in all the areas surrounding
767 the volcano. This appears to be an important piece of information, indicating a broadening of the area
768 affected by intense degassing, (Francisconi et al., 2019). In 1475, another seismic phase was reported
769 (Guidoboni, 2020), with maximum intensity $I_0 = IV - V$. Over the following twenty years, ground
770 uplift continued at an accelerated rate. This period culminated with a strong seismic phase occurring
771 in October 1498, reaching considerable maximum intensity ($I_0 = VII$). A low-intensity seismic phase
772 then followed during the period 1499 - 1503 (maximum intensity $I_0 = V$) (Fig. 19a – interval A).
773 Such a long-term precursory phase could likely be interpreted as mainly due to intense degassing,
774 coming from the deep magma chamber and progressively increasing pressure in the shallow layers
775 of the geothermal system, without significant contribution from direct magma intrusion at shallow
776 depth.

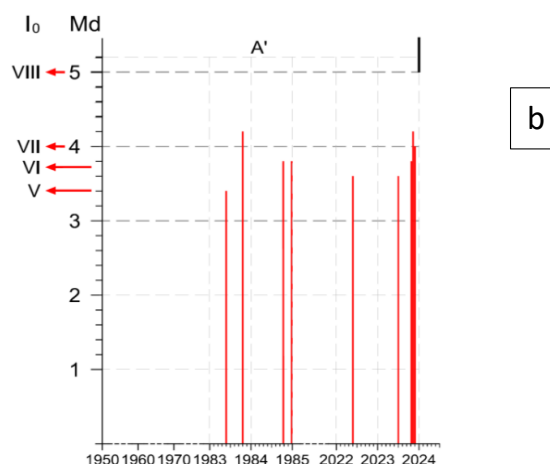
777 - After this first initial long-term precursory phase, a new phase of *medium-term precursors* followed.
778 This phase was characterized by stronger seismic events in 1505 and 1508, which were of higher



779 intensity with respect to the previous ones (maximum intensity $I_0 = VIII$) (Guidoboni and Ciuccarelli,
780 2011). Additionally, there was a faster ground uplift during this period, resulting in serious damage
781 to buildings and several casualties. This seismic phase could have been caused by either a higher
782 stress associated with increased uplift level, or magma intrusion, from the deep magma chamber into
783 shallower levels. This intrusion could have produced higher stress resulting in seismic activity of
784 greater intensity. Although it is obviously difficult to identify, from historic sources alone, the
785 respective roles of the deep degassing into the hydrothermal system versus shallow magma intrusion,
786 we believe that the reported evidence of vegetation damage and increased degassing in the first phase,
787 and the increase of earthquake intensity in the second phase, indicate respectively a main contribution
788 of degassing perturbing the hydrothermal system, in the first phase, and shallow magma intrusion in
789 the second phase. This phase concluded in 1520, with a medium intensity earthquake ($I_0 = V-VI$)
790 (Fig. 19a – interval B), likely again associated with perturbations in the hydrothermal system.
791
792



793



794

795 **Fig. 19 – a) Reported earthquakes occurred before and after the 1538 eruption (from**
 796 **Guidoboni and Ciuccarelli, 2011). The computed intensities of these earthquakes have been**
 797 **converted in magnitudes using the considerations made in the text. b) Highest magnitude**
 798 **earthquakes ($M \geq 3.5$) occurred since 1950 to present.**

799

800 - After 16 years of relative seismic quiescence, likely characterized by low-intensity earthquakes not
 801 reported in chronicles, a short-term precursory phase began in 1536. It commenced with continuous
 802 seismicity, without major damage ($I_o = III - IV$), continuing with similar features until the early 1537.
 803 It is possible that this last seismic phase, characterized by relatively low magnitude, was caused by
 804 low-frequency seismicity, resulting from magma oscillations during the fractures opening (see
 805 Chouet, 1996). This seismicity became more frequent just before the eruption. In February of the
 806 same year, the seismic activity peaked with stronger events ($I_o = VI - VII$), accompanied by an
 807 increase in the fumarolic activity at Solfatara. This provides clear evidence that this seismicity was
 808 again related to perturbations in the hydrothermal system. A final increase in seismic activity ($I_o =$
 809 $VIII$), began in mid-June 1538, accompanied by a 7-meter ground uplift at the eruption site, located
 810 3 km away from the center of previous maximum uplift. (Fig. 19a – interval C) (Parascandola, 1943,
 811 Rolandi et al., 1986; Guidoboni and Ciuccarelli, 2011; Guidoboni, 2020). The claim made by Di Vito
 812 et al. (2016) regarding very large local uplift at the eruption site, exceeding 18 m., appears to be
 813 inaccurate. Historical chronicles from the time indicate that the Roman road ‘Via Herculea’, which
 814 was submerged during the subsidence phase and was at about 7 m of depth in 1430, did not re-emerge
 815 during or after the 1538 eruption. Given the proximity of the Via Herculea to the 1538 vent, this
 816 suggests that local uplift there should not have exceeded ca. 7 m.



817 - On 1538, approximately 0.03 km³ of emitted products, through phreatomagmatic activity with low
818 mechanical efficiency (Rolandi et al., 2023). After six days the eruption resumed with Strombolian-
819 type magmatic activity, mantling the tuff cone with a 0.5 m thick blanket of dark trachytic scoria. The
820 final phase of activity ended with the collapse of the Strombolian eruptive column, resulting in the
821 deposition of a scoria flow in a depression on the south-east side. Monte Nuovo has been the second
822 smallest volcanic eruption (and volcanic edifice) of the post-caldera activity, with VEI = 2 (Rolandi
823 et al., 2023).

824

825 **6.3 The post-eruption seismicity**

826 We will now consider the seismic phase following the eruption just described which we will indicate
827 as the *aftereffect of the 1538 eruption*. This phase was likely triggered by continuing degassing from
828 the deep magma chamber, and/or by new episodes of shallow magma intrusion not reaching the
829 surface to erupt. It began in 1564 with earthquakes of medium intensity ($I_0 = V - VI$), followed by a
830 phase of lower intensity 2 years later. In 1570 seismic intensity increased ($I_0 = VI - VII$), causing
831 damage to the buildings of the city of Pozzuoli. Between 1575 and 1580 a new phase of low seismic
832 intensity began, culminating, in 1582, with two earthquakes, respectively of intensity $I_0 = VII - VIII$.
833 These earthquakes caused partial collapses in several houses and serious damage to churches and
834 buildings, as well as numerous casualties (Parascandola, 1943; Guidoboni e Cucciarelli, 2010;
835 Guidoboni, 2020).

836

837 **7. Comparison of precursory phases of 1538 eruption with current unrest**

838 This study is mainly aimed at understanding how the evolution of the ground movement phases linked
839 to the 1538 eruption can help build realistic scenarios for the evolution of the same recent phases at
840 the Campi Flegrei caldera. Common features between the medieval and present-day ground movement
841 phases are described in the following:

842 The main similarity is that the seismicity, in the past and in the recent unrest, has been clearly correlated
843 both with the total uplift and the uplift rate; it is practically absent in periods of subsidence (Dvorak
844 and Gasparini, 1991; Kilburn et al., 2017; Troise et al., 2019).

845 We found, in particular, that seismicity of period 1950-2024 is on the same order than the period
846 1430-1503, whereas the latter, as we have previously observed, was the first phase of preparation of
847 the 1538 eruption. Although the total amount of uplift in the period 1430-1503, about 10 m, was more
848 than double than the total uplift recorded since 1950-2023, of about 4.1 m., the seismicity in the two
849 periods has been remarkably comparable. The maximum magnitude, $M=4.2$ recently occurred on



850 October 2nd, 2023, is in fact very similar to the maximum magnitude reconstructed for the period
851 1430-1503 (Fig.19a interval A and Fig.19b interval A’).

852 Another common feature is that both seismic phases can be mostly ascribed to the effect of
853 pressurized hydrothermal fluids. So, till now there is a close analogy between the ‘long term
854 precursory phase’ preceding the 1538 eruption and the recent unrest 1950-2023; the only clear
855 difference is, as we already noted, the much lower cumulative uplift of the recent unrest.

856 Such observations led us to consider two possible scenarios for the evolution of the present unrest.

857

858 **7.1 First scenario**

859 The first scenario would imply that the present unrest progresses towards a new eruption. Although
860 there is, presently, no evidence for shallow magma intrusions occurring during the present unrest
861 since 2006 (see Moretti et al., 2017, 2018; Troise et al., 2019), a new shallow magma intrusion, in
862 the near future, cannot be ruled out. Another possibility is that the mush, which should be present at
863 low depth, could be re-mobilised by hot fluids coming from the main magma chamber. Troise et al.
864 (2019), showed in fact evidence for a likely shallow magma intrusion occurred at about 3 km of depth,
865 during the 1982-1984 unrest, with a volume of about 0.03 km³, i.e. the same order of magnitude of
866 the erupted volume in the 1538 event. The same authors calculated that such a sill intrusion should
867 have solidified, in form of mush, after about 20 years, i.e. around 2003. If the actual unrest will
868 progress towards an eruption, it is also very likely that seismicity will increase, in frequency and
869 magnitude, possibly reaching magnitudes around 5 or even higher. Earthquakes of magnitude 5, in
870 this area, would occur at very shallow depths (not higher than about 3 km), so producing high
871 intensities (higher than VIII MCS, see Fig. 19). Finally, from a civil protection perspective, we must
872 also take into account the possible onset of a post-eruptive seismic phase, which after the 1538
873 eruption lasted about 40 years. In conjunction with the prefigured scenario, the problem of forecasting
874 the position of a new eruptive vent is also extremely relevant because, in principle, it could be opening
875 in any sector of the caldera. Despite the indications contained in several probabilistic studies on the
876 subject (Alberico et al., 2002; Selva et al., 2011), we must consider they are biased by the assumption
877 of stationary conditions, which is implied in any probability computation based on the frequency of
878 past events. As the most evident example that such probabilistic determinations have a poor
879 reliability, it is enough to note that, on the basis of such calculations, the site of the 1538 Monte
880 Nuovo eruption would have never been predicted. The most reliable indication of the most likely
881 future vent could come from the most seismic areas, because they reflect the areas of maximum shear
882 stress. In this perspective, the Solfatara-Agnano area (see Fig. 15a), which is by far the most
883 seismically active, could be the most probable site for future vent opening. However, the most



884 effective way to address this problem would be the prompt determination of localized uplift in
885 addition to the usual bell-shaped one centered on Pozzuoli harbor. Although some recent eruptions
886 (e.g. at Hekla volcano: Wonderman, 2000) show that the rise of magma from several km to the surface
887 can be so fast to be practically useless for civil protection purposes, localized and considerable
888 ground uplift was actually observed well before (months or years) the 1538 eruption, making it likely
889 that this precursor will be observed before any future eruptions in the area.

890 We should however mention the possibility that, even without new shallow magma intrusions, and/or
891 in absence of mobilized mush eruption, the increase of pressure for aquifer heating above the critical
892 threshold could produce a phreatic eruption. Phreatic eruptions are in general very difficult to
893 forecast, and also to detect from the past geological record. However, there is some robust indication
894 for at least one phreatic eruption occurred in the area, in 1198 (Scandone et al., 2010).

895

896 **7.2 Second scenario**

897 As an alternative scenario, we should consider the one which stops sometimes without evolving
898 towards an eruption. Despite the similarity of the recent unrest with the first phase leading to the 1538
899 eruption, we could in fact consider the notable difference in the cumulative uplift between the past
900 and present unrests: 10 m., as compared with 4.1 m. The level of ground uplift is critical, because it
901 indicates the level of stress accumulated underground. As pointed out by Kilburn et al. (2017), when
902 the level of stress reaches a critical value, the medium rheology becomes totally fragile and any small
903 amount of incremental stress can cause the collapse (i.e. the catastrophic fracturing) of the shallow
904 crust, thus producing the eruption. Actually, we don't know the critical stress level for the shallow
905 crust at Campi Flegrei. Kilburn et al. (2023) claimed, from the observation of the trend of cumulative
906 number of earthquakes as a function of cumulative uplift, that such critical value would have been
907 reached and overcome in 2015. However, looking at the data they present, no reliable change in the
908 trend of seismicity after 2015 can be really observed; furthermore, their assumption that the maximum
909 internal stress reached in 1984 has been overcome in 2015 is not justified, because only in June 2022
910 the maximum ground level reached the same maximum value of 1984 (Osservatorio Vesuviano,
911 2022). Besides any speculation, it is clear that, if the internal stress had really overcome the critical
912 level in 2015, considering the large additional uplift cumulated since then (about 0.85 m.), and hence
913 the considerable incremental stress, the system would have already been collapsed, and an eruption
914 occurred. The very high deformation occurred before the 1538, namely 16 m plus the localized uplift
915 occurred just at the vent site before the eruption, seems to indicate that the critical stress level is much
916 higher than the one presently reached. Therefore, there is a possibility that the progression towards



917 eruption conditions is too gradual to culminate in an actual eruption, and the unrest may cease before
918 reaching that point.

919 8. Conclusion

920 In this paper, we have presented a detailed reconstruction of the ground deformation, and a
921 comprehensive analysis of the main observations characterizing the events before, during and after the
922 1538 Monte Nuovo eruption, the only eruption occurred at Campi Flegrei caldera in historical times.
923 This reconstruction has allowed us to correct some widely diffused but erroneous reconstructions,
924 found in the past and recent literature, based on clear historical evidence. Specifically, we
925 demonstrated that subsidence in the area began during the Greek colonization (VIII century BC) and
926 persisted through Roman times, with documentation dating back to 90 BC. Additionally, we
927 reconstructed the evolution of ground deformation at Pozzuoli harbor during the Middle Age,
928 demonstrating that maximum subsidence occurred around 1430. We also tracked the ground level from
929 1430 until the first half of the 19th century, using historical data on the height of the Serapeum floor
930 relative to sea level.

931 Furthermore, by reconstructing the subsidence and uplift of the Via Herculea, based on ancient
932 chronicles, we provided clear evidence indicating that the local uplift preceding the eruption at the
933 Monte Nuovo site, situated near Via Herculea, did not exceed 5-7 meters. This evidence disproves
934 claims in recent literature (Di Vito et al., 2016), that suggested local uplift around M. Nuovo, reached
935 elevations as high as 19 m immediately before the eruption.

936 Our reconstruction of geophysical anomalies (mainly ground displacement and seismicity) preceding
937 and following the 1538 eruption has been tentatively interpreted in comparison with observations and
938 data collected during the recent unrests. This approach has enabled the formulation of two possible
939 scenarios for the evolution of the present unrest, which, so far, has shown notable similarities to the
940 long-term precursors of the 1538 eruption.

941 The first scenario involves the progression of phenomena towards an eruption, suggesting that, in the
942 near future, earthquakes with magnitude up to 5 or slightly higher may occur, both preceding the
943 eruption and persisting for several decades afterward. Conversely, the alternative scenario, implies that
944 the unrest may cease before an eruption occurs. This possibility is supported by the fact that ground
945 uplift observed from 1950 to 2023, compared with the uplift occurred over an equivalent period from
946 1430 to 1503, is significantly lower (4.1 m as compared to 10 m). Since the overpressure in the system
947 is somewhat proportional to the amount of uplift, it is plausible that the recent unrest has not reached
948 the critical value for catastrophic fracture of shallow rocks. In addition, if cumulative stress increases
949 too slowly, a substantial amount of previous stress can be cleared depending on viscoelastic relaxation
950 and its characteristic times. While the exact critical threshold and viscoelastic relaxation time remain



951 unknown, they can be tentatively inferred from the maximum deformation observed before the 1538
952 eruption. The bell-shaped cumulative vertical displacement centered at Pozzuoli, before the 1538
953 eruption, was much larger, reaching 16 m., compared to the about 4 m recorded from 1950 to 2023.
954 This substantial difference, assuming the rheology and strength of shallow rocks in the 0-3 km depth
955 range remain unchanged, suggest that we are currently far from reaching the critical stress threshold
956 necessary for an eruption.

957

958 **Data availability**

959 All raw data can be provided by the corresponding authors upon request.

960

961 **Author contributions**

962 GR, GDN and CT analyzed historical and volcanological data; GDN and CT analyzed earthquake
963 intensity/magnitude data; MS analyzed seismic data; GR, MS and MDL wrote the manuscript draft
964 and prepared the figures; GDN, CT and MS reviewed and edited the manuscript.

965

966 **Competing interests**

967 The authors declare that they have no conflict of interest.

968

969 **Acknowledgments**

970 The authors want to thank Prof. Marina Petrone who helped to recover some important Middle Age
971 references on Campi Flegrei.

972

973

974 **References**

975 AGIP, 1987. Geologia e geofisica del sistema geotermico dei Campi Flegrei. Servizi Centrali per
976 l'Esplorazione, SERG-MMESG, San Donato

977 Alberico, I., Petrosino, P., and Lirer, L., 2011. Volcanic hazard and risk assessment in a multi-source
978 volcanic area: the example of Napoli city (Southern Italy), *Nat. Hazards Earth Syst. Sci.*, 11, 1057–
979 1070, <https://doi.org/10.5194/nhess-11-1057-2011>, 2011.

980 Altaner, S., Demosthenous, C., Pozzuoli, A., Rolandi, G., 2013. Alteration history of Mount Epomeo
981 Green Tuff and a related polymictic breccia, Ischia Island, Italy: Evidence for debris avalanches.
982 *Bulletin of Volcanology* 75, 5, <https://doi.org/10.1007/s00445-013-0718-1>



- 983 Amato, L. and Gialanella, C., 2013. New evidences on the Phlegraean bradyseism in the area of
984 Puteolis harbour. Conference: Geotechnical Engineering for the Preservation of Monuments and
985 Historic Sites. <https://doi.org/10.13140/2.1.2326.0482>
- 986 Anecchino, R., 1931. Agnano, l'origine del nome e del lago. *Bollettino Flegreo*, 5.
987
- 988 Aster, R. and Meyer, R., 1988. Three-dimensional velocity structure and hypocenter distribution in
989 the Campi Flegrei caldera, Italy. *Tectonophysics*, 149, 195–218
990
- 991 Aucelli, P.C. et al., 2020. Ancient Coastal Changes Due to Ground Movements and Human
992 Interventions in the Roman Portus Julius (Pozzuoli Gulf, Italy): Results from Photogrammetric and
993 Direct Surveys. *Water*, 12, 658. <https://doi.org/10.3390/w1203065>
- 994 Bachmann, O., Bergantz, G.W., 2006. Gas percolation in upper-crustal silicic crystal mushes as a
995 mechanism for upward heat advection and rejuvenation of near-solidus magma bodies. *Journ.*
996 *Volcanol. and Geoth. Res.*, 149, 85-102
997
- 998 Bachmann, O., Huber, C., 2016. Silicic mushes reservoirs in the Earth's crust. *American*
999 *Mineralogist*, 101, 11, 2377–2404. <https://doi.org/10.2138/am-2016-5675>
1000
- 1001 Barberi, F., Corrado, G., Innocenti, F., Luongo, G., 1984. Phlegraean Fields 1982–1984: Brief
1002 Chronicle of a Volcano Emergency in a Densely Populated Area. *Bull. Volcanol.*, 47-2, 175-185.
- 1003 Bergantz, G.W., 1989. Underplating and partial melting: implications for melt generation and
1004 extraction. *Science* <https://doi.org/10.1126/science.245.4922.1093>
- 1005 Brahm, R., Parada, M.A., Morgado, E.E., Contreras, C., 2015. Pre-eruptive rejuvenations of
1006 crystalline mush by reservoir heating: the case of trachy-dacitic lavas of Quetrupillán Volcanic
1007 Complex, Chile (39°30' lat. S). *American Geophysical Union, Fall Meeting 2015*, abstract id. V43B-
1008 3122, Bibcode: 2015AGUFM.V43B3122B
1009
- 1010 Burgisser, A., Bergantz, G.W., 201. A rapid mechanism to remobilize and homogenize crystalline
1011 magma bodies. *Nature* 471(7337):212-5, <https://doi.org/10.1038/nature09799>
1012



- 1013 Battaglia, J., Zollo, A. Virieux, J., Dello Iacono, D., 2008. Merging active and passive data sets in
1014 travelttime tomography: The case study of Campi Flegrei caldera (Southern Italy) Geophysical
1015 Prospecting, 56, 555–573 <https://doi.org/10.1111/j.1365-2478.2007.00687.x>
- 1016 Bellucci, F., Woo, J., Kilburn, C. R. J. & Rolandi, G., 2006. In Mechanisms of Activity and Unrest
1017 at Large Calderas Vol. 269 (eds. Troise C., De Natale, G. & Kilburn, C.R.J.) The Geological Society
1018 of London Special Publication, 141–158.
- 1019 Beauducel, F., De Natale, G., Obrizzo, F., Pingue, F., 2004. 3-D modelling of Campi Flegrei ground
1020 deformations: role of caldera boundary discontinuities. Pure Appl. Geophys., 161.
- 1021 Boccaccio, G., 1355-1373. De Montibus.
- 1022 Bodnar, R. J., Cannatelli, C., de Vivo, B., Lima, A., Belkin, H.E., Milia, A., 2007. Quantitative model
1023 for magma degassing and ground deformation (bradyseism) at Campi Flegrei, Italy: implications for
1024 future eruptions, *Geology*, 35, 9, pp. 791–794.
- 1025 Calò, M., Tramelli, A., 2018. Anatomy of the Campi Flegrei caldera using enhanced seismic
1026 tomography models, *Scientific Reports*, 8, 1, 16254.
- 1027 Camodeca, G., 1987. Le antichità di Pozzuoli, la Ripa Puteolana e i resti sommersi del Porto Giulio,
1028 G. Macchiaroli Editore, Napoli.
- 1029 Cannatelli, C., Spera, F.J., Bodnar, R.J., Lima, A., De Vivo, B., 2020. Ground movement
1030 (bradyseism) in the Campi Flegrei volcanic area: a review. In: “Vesuvius, Campi Flegrei, and
1031 Campanian volcanism”, In: De Vivo B., Belkin H. E & Rolandi G., Eds, Elsevier, 15, 407-433. ISBN:
1032 978-0-128-16454-9.
- 1033
- 1034 Cappelletti, P., Petrosino, P., De Gennaro, M., Colella, A., Graziano, S.F., D’Amore, M., Mercurio,
1035 M., Cerri, G., De Gennaro, R., Rapisardo, G., Langella, A., 2015. The “Tufo Giallo della Via
1036 Tiberina” (Sabatini Volcanic District, Central Italy): a complex system of lithification in a pyroclastic
1037 current deposit. *Mineralogy and Petrology*, 109 (1) 85-101 <https://doi.org/10.1007/s00710-014-0357->
1038 z
- 1039
- 1040 Carrara, A., Burgisser, A., Bergantz, G.W., 2020. The architecture of intrusions in magmatic mush.
1041 *Earth and Planetary Science Letters*, 549, 1, 116539.



- 1042 Caricchi, L., Annen, C., Blundy, J.D., Simpson, G., Pinel, V., 2014. Frequency and magnitude of
1043 volcanic eruptions controlled by magma injection and buoyancy. *Nature Geoscience*, 7, 126–
1044 130. <https://doi.org/10.1038/ngeo2041>.
- 1045 Caruso, M., 2004. Il territorio puteolano fra età romana e alto Medioevo. *Bollettino Flegreo*, Terza
1046 serie, N°17
- 1047 Cashman, K.V., Sparks, R.S.J., Blundy, J., 2017. Vertically extensive and unstable crystals mushes:
1048 a unifying view of igneous processes associated with volcanoes. *Science* 355, 6331,
1049 <https://doi.org/10.1126/science.aag3055>
- 1050 Charlton, D., Kilburn, C., Edwards, S., 2020. Volcanic unrest scenarios and impact assessment at
1051 Campi Flegrei caldera, Southern Italy. *Journal of Applied Volcanology*, 9, 7 (DOI).
- 1052
- 1053 Chiodini, G., Caliro, S., Avino, R. et al., 2021. Hydrothermal pressure-temperature control on CO₂
1054 emissions and seismicity at Campi Flegrei (Italy),” *Journal of Volcanology and Geothermal Research*,
1055 414, 107245. <https://doi.org/10.1016/j.jvolgeores.2021.107245>.
- 1056
- 1057 Chouet, B. A. (1996). Long-period volcano seismicity: its source and use in eruption
1058 forecasting. *Nature*, 380, 6572, 309-316. <https://doi.org/10.1038/380309a0>
- 1059
- 1060 Cinque, A., Rolandi, G., Zamparelli, V., 1983. L’estensione dei depositi marini olocenici
1061 nei Campi Flegrei in relazione alla vulcanotettonica. *Boll. Soc. Geol. It.*, 104, 327e348
- 1062
- 1063 Colletta, T., 1988. Pozzuoli, città fortificata in epoca vicereale - Storia dell’Urbanistica/Campania 1-
1064 Pozzuoli. Pubblicazione semestrale diretta da E. Guidoni. Supplemento Luglio-Dicembre
- 1065
- 1066 Costa, A., Di Vito, M.A., Ricciardi, G.P., Smith, V. C., Talamo, P., 2022. The long and intertwined
1067 record of humans and the Campi Flegrei volcano (Italy). *Bulletin of Volcanology*, 84, 5.
1068 <https://doi.org/10.1007/s00445-021-01503->
- 1069 D’Antonio, M., Civetta, L., Orsi, G., Pappalardo, L., Piochi, M., Carandente, A., De Vita, S.,
1070 Di Vito, M.A., Isaia, R., 1999. The present state of the magmatic system of the Campi Flegrei
1071 caldera based on a reconstruction of its behavior in the past 12 ka. *J. Volcanol. Geotherm.*
1072 *Res.*, 91, 2-4, 247-268.



- 1073 De Jorio, A., 1820. Ricerche sul Tempio de Serapide in Pozzuoli, Monumenti inediti di Antichità e
1074 Belle Arti, Napoli.
- 1075 Del Gaudio, C., Aquino, I., Ricciardi, G.P., Ricco, C., Scandone, R., 2010. Unrest episodes at Campi
1076 Flegrei: A reconstruction of vertical ground movements during 1905–2009. *Journal of Volcanology
1077 and Geothermal Research* 195, 1, 48-56. <https://doi.org/10.1016/j.jvolgeores.2010.05.014>
- 1078 De Natale, G., Zollo, A., 1986. Statistical analysis and clustering features of the Phlegraean Fields
1079 earthquake sequence (May 1983-May 1984). *Bull. Seism. Soc. Am.*, 76, 3, 801–814.
1080 <https://doi.org/10.1785/BSSA0760030801>
1081
- 1082 De Natale, G., Pingue, F., Allard, P. and Zollo, A., 1991. Geophysical and geochemical modeling of
1083 the Campi Flegrei caldera. In '*Campi flegrei*' (G. Luongo R. Scandone eds.), *J. Volcanol. Geotherm.
1084 Res.*, 48, 199–222.
1085
- 1086 De Natale, G., Pingue, F., 1993. Ground deformations in collapsed caldera structures. *Journal of
1087 Volcanology and Geothermal Research*, 57, 1-2, 19-38.
1088
- 1089 De Natale, G., Petrazzuoli, S.M., Pingue, F., 1997. The effect of collapse structures on ground
1090 deformations in calderas. *Geophysical Research Letters*, 24, 1555–1558.
1091
- 1092 De Natale, G., Troise, C., Pingue, F., 2001. A mechanical fluid-dynamical model for ground
1093 movements at Campi Flegrei caldera. *J. Geodyn.*, 32, 487-517.
1094
- 1095 De Natale, G., Kuznetov, I., Krondrod, T., Peresan, A., Sarao, A., Troise, C., Panza, G.F., 2004.
1096 Three decades of seismic activity at Mt. Vesuvius: 1972-2000. *Pure Appl. Geophys.*, 161, 1, 123-
1097 144. <https://doi.org/10.1007/s00024-003-2430-0>
1098
- 1099 De Natale, G., Troise, C., Pingue, F., Mastrolorenzo, G., Pappalardo, L., Battaglia, M., Boschi, E.,
1100 2006b. The Campi Flegrei caldera: Unrest mechanisms and hazards. (London: Geological Society)
1101 *Geol. Soc. London Spec. pub.*, 269, 1. <https://doi.org/10.1144/GSL.SP.2006.269.01.03>.
1102



- 1103 De Natale, G., Troise, C., Mark, D., Mormone, A., Piochi, M., Di Vito, M.A., Isaia, R., Carlino, S.,
1104 Barra., D., Somma, R., 2016. The Campi Flegrei Deep Drilling Project (CFDDP): New insight on
1105 caldera structure, evolution and hazard implications for the Naples area (Southern Italy).
1106 Geochemistry, Geophysics, Geosystem, <https://doi.org/10.1002/2015GC00618341>.
1107
- 1108 De Natale, G., Petrazzuoli, S., Romanelli, F., Troise, C., Vaccari, F., Somma, R., Peresan, A., Panza,
1109 G.F., 2019. Seismic risk mitigation at Ischia island (Naples, Southern Italy): an innovative approach
1110 to mitigate catastrophic scenarios. Eng. Geol., 261, 105285.
1111
- 1112 Di Bonito, R., Giamminelli, R., 1992. Le Terme dei Campi Flegrei, Topografia Storica. Jandi Sapi
1113 Editori, Milano-Roma.
1114
- 1115 Di Girolamo, P., Ghiara, M.R., Lirer, L., Munno, R., Rolandi, G., Stanzione, D., 1984.
1116 Vulcanologia e petrologia dei Campi Flegrei. Boll. Soc. Geol. Ital., 103.
1117
- 1118 Di Vito, M.A., Lirer, L., Mastrolorenzo, G., Rolandi G., 1987. The Monte Nuovo eruption (Campi
1119 Flegrei, Italy). Bulletin of Volcanology 49, 608–615.
- 1120 Di Vito, M.A., Isaia, R., Orsi, G., Southon, J., De Vita, S., D’Antonio, M., Pappalardo, L., Piochi,
1121 M., 1999. Volcanism and deformations since 12.000 years at Campi Flegrei caldera
- 1122 Di Vito, M.A., Arienzo, I., Braia, G., Civetta, L., D’Antonio, M., Di Renzo, V., Orsi, G., 2011. The
1123 Averno 2 fssure eruption: a recent small-size explosive event at the Campi Flegrei caldera (Italy).
1124 Bull. Volcanol 73:295–320. <https://doi.org/10.1007/s00445-010-0417>
- 1125 Di Vito, M.A., Acocella, V., Aiello, G., Barra, D., Battaglia, M., Carandente, A., Del Gaudio, C., S.
1126 de Vita, S., GP Ricciardi, G.P., Ricco, C., Scandone, R., Terrasi, F., 2016. Scientific Reports, 6,
1127 Article number: 32245. <http://www.nature.com/articles/srep32245>
- 1128 Dvorak, J.J. and Gasparini, P., 1991. History of earthquakes and vertical ground movement in Campi
1129 Flegrei caldera, Southern Italy: comparison of precursory events to the A.D. 1538 eruption of Monte
1130 Nuovo and of activity since 1968. Journ. Volc. Geoth. Res., 48, 1-2.
1131
- 1132 Dvorak, J.J., Mastrolorenzo, G., 1991. The mechanism of recent movements in Campi Flegrei
1133 caldera, Southern Italy. Geologic Society of America special paper, 263.



- 1134 Druitt, T.H., Sparks, R.S.J., 1984. On the formation of calderas during ignimbrite eruptions. *Nature*,
1135 310, 679-681.
- 1136 Edmonds, M., Cashman, K. V., Holness, M., Jackson, M., 2019. Architecture and dynamics of
1137 magma reservoirs. *Phil. Trans. Royal Soc., Mat. Phis. and engeener. Sci.*, 377, 2139.
1138 <https://doi.org/10.1098/rsta.2018.0298>
- 1139
- 1140 Folch, A., Gottsmann, J., 2006. Faults and ground uplift at active calderas, Geological Society,
1141 London, Special Publications, 269, 109–120.
- 1142
- 1143 Fournier, R.O., 1999. Hydrothermal processes related to movement of fluid from plastic into brittle
1144 rock in the magmatic epithermal environment, *Econ. Geol.*, 94, 8, 1193-1211.
- 1145
- 1146 Francisconi, G., Todesco, M., Ciuccarelli, C., 2019. Storia del Monte Nuovo. L'ultima eruzione dei
1147 Campi Flegrei. INGV Vulcani.
- 1148
- 1149 Franco, E., 1974. La zeolitizzazione naturale: in zeoliti e zeolitizzazione. *Atti Convegni Licei*, 33-60
- 1150
- 1151 Fuiano, M., 1951. Niccolò Jamsilla. *Atti dell'Accademia Pontaniana. Nuova serie, Volume 3 – Anno
1152 Accademico 1949 -50 – Napoli - Stabilimento tipografico Giannini*
- 1152 Gaeta, F.S., Peluso, F., Milano, G., Arienzo, I., 2002. A Physical Appraisal of A New Aspect of
1153 Bradyseism: The Mini-uplifts. *Journal of Geophysical Research Atmospheres* 108(B8)
1154 <https://doi.org/10.1029/2002JB001913>
- 1155
- 1156 Gianfrotta, P.A., 1993. Puteoli sommersa, in F. Zevi (a cura di), *Puteoli: 115-124*. Napoli, Banco di
1157 Napoli.
- 1158 Gudmundsson, A., 2012. Magma chambers: Formation, local stresses, excess pressures, and
1159 compartments. *Jour. Volcanol. Geoth. Res.*, <https://doi.org/10.1016/j.jvolgeores.2012.05.015>
- 1160
- 1161 Guidoboni, E., Ciuccarelli, C., 2011. The Campi Flegrei caldera: historical revision and new data on
1162 seismic crises, bradyseisms, the Monte Nuovo eruption and ensuing earthquakes (twelfth century
1163 1582 AD), *Bulletin of Volcanology*, 73, 6, pp. 655-677, <https://doi.org/10.1007/s00445-010-0430-3>



- 1164 Guidoboni, E., 2020. Pozzuoli - terremoti e fenomeni vulcanici nel lungo periodo. a cura di AISI-
1165 Associazione Italiana di Storia dell'Ingegneria - VIII Convegno di Storia dell'Ingegneria, Napoli,
1166 Volume I
- 1167 Gretener, P.E., 1969. On the mechanics of the intrusion of sills. *Canadian Journal of Earth Sciences*,
1168 6, 6.
- 1169 Guthier, V., 1912. Il Bradisisma Flegreo all'epoca ellenica. *Rend. Real Accad. Sci, Fis. e Mat. Napoli*,
1170 Serie III, Vol. XVIII, Anno LI, 91-94.
1171
- 1172 Johnson, E.R., Wallace, P.J., Cashman, K.V., Granados, H.D., Kent, A.J.R., 2008. Magmatic volatile
1173 contents and degassing-induced crystallization at Volcán Jorullo, Mexico: Implications for melt
1174 evolution and the plumbing systems of monogenetic volcanoes. *Earth Plan. Sci. Lett.*, 269, 477
1175
- 1176 Kilburn, C.R.J., De Natale, G., Carlino, S., 2017. Progressive approach to eruption at Campi Flegrei
1177 caldera in southern Italy. *Nature Communications*, 8, 15312
- 1178 Kilburn, C.R.J., Carlino, S., Danesi, S., Pino, N.A., 2023. Potential for rupture before eruption at
1179 Campi Flegrei caldera, Southern Italy. *Commun. Earth Environ.*, 4, 190.
1180 <https://doi.org/10.1038/s43247-023-00842-1>
- 1181 Lanzarin, O., 2021. Trugli dei bagni di Pozzuoli. Immagine e fortuna di due edifici termali antichi.
1182 <https://doi.org/10.17401/lexicon.33.2021-i>
- 1183 Lima, A., De Vivo, B., Spera, F.J. et al., Bodnar, M., Milia, A., Nunziata, C., Belkin, H., Cannatelli,
1184 C., 2009. Thermodynamic model for uplift and deflation episodes (bradyseism) associated with
1185 magmatic-hydrothermal activity at the Campi Flegrei (Italy). *Earth Sci. Rev.*, 97, 1-4, 44–58.
- 1186 Lima, A. Bodnar, R.J., De Vivo, B., Spera, F. J., Belkin, H.E., 2021. Interpretation of Recent Unrest
1187 Events (Bradyseism) at Campi Flegrei, Napoli (Italy): Comparison of Models Based on Cyclical
1188 Hydrothermal Events versus Shallow Magmatic Intrusive Events. *Geofluids* , 2000255.
1189 <https://doi.org/10.1155/2021/2000255>
1190
- 1191 Mancusi, F., 1987. Campi Flegrei. Sergio Civita Editore, Napoli.
1192



- 1193 Marti, J., Lopez, C., Bartolini, S., Becerrill, L., 2016. Stress control of monogenic volcanism: A
1194 review. *Front. Earth Sci., Sec. Volcanology*, 4
1195
- 1196 Marturano, A., Esposito, E., Porfido, S., Luongo, G., 1988. Il terremoto del 4 Ottobre 1983
1197 (Pozzuoli): Attenuazione dell'intensità con la distanza e relazione magnitudo-Intensità, zonazione
1198 della città di Napoli. *Mem. Soc. Geol. It.*, 41, 941-948
1199
- 1200 Marsh, B.D., 1989. Magma chambers. *Ann. Rev. Earth Planet Sci.* 17, 439–474.
1201 <https://doi.org/10.1146/annurev.ea.17.050189.002255>
1202
- 1203 Milana, G., De Sortis, A., Rovelli, A., 2010. Contenuto in bassa frequenza nei terremoti vulcanici del
1204 Monte Etna e danneggiamento degli edifici. Fascicolo N.2: Progettazione Sismica, Sezione Articoli
1205
- 1206 Moretti, R., De Natale, G., Troise, C., 2017. A geochemical and geophysical reappraisal to the
1207 significance of the recent unrest at Campi Flegrei caldera (Southern Italy). *Geochemistry,*
1208 *Geophysics, Geosystems*, <https://doi.org/10.1002/2016GC006569>
1209
- 1210 Moretti, R., Troise, C., Sarno, F., De Natale, G., 2018. Caldera unrest driven by CO₂-induced drying
1211 of the deep hydrothermal system, *Scientific Reports G.*, 8, 1, 8309
1212
- 1213 Morhange, C., Marriner, N., Laborel, J., Todesco, M., & Oberlin, C., 2006. Rapid sea-level
1214 movements and noneruptive crustal deformations in the Phlegrean fields caldera,
1215 Italy. *Geology*, [34\(2\)](https://doi.org/10.1130/G21894.1), 93–96. <https://doi.org/10.1130/G21894.1>
1216
- 1217 Nespoli, F. et al., 2023. A reduced-turbulence regime in the Large Helical Device upon injection
1218 of low-Z materials powders. *Nucl. Fusion*, 63 076001. <https://doi.org/10.1088/174-4326/acd465>
1219
- 1220 Niccolini, A., 1846. *La gran terma puteolana*. Napoli
1221
- 1222 Osservatorio Vesuviano, 2022. *Bollettino Mensile Campi Flegrei 2022 06* (In Italian).
1223 [https://www.ov.ingv.it/index.php/monitoraggio-e-infrastrutture/bollettini-tutti/mensili-dei-vulcani-](https://www.ov.ingv.it/index.php/monitoraggio-e-infrastrutture/bollettini-tutti/mensili-dei-vulcani-della-campania/flegrei/anno-2022-2/1114-bollettino-mensile-campi-flegrei-2022-06/file)
1224 [della-campania/flegrei/anno-2022-2/1114-bollettino-mensile-campi-flegrei-2022-06/file](https://www.ov.ingv.it/index.php/monitoraggio-e-infrastrutture/bollettini-tutti/mensili-dei-vulcani-della-campania/flegrei/anno-2022-2/1114-bollettino-mensile-campi-flegrei-2022-06/file)
1225



- 1226 Parascandola, A., 1943. Il Monte Nuovo ed il Lago Lucrino, in *Bollettino della Società dei Naturalisti*
1227 in Napoli, Volumi 1944–1946, 55, 151-312. Stab. tip. G. Genovese
1228
- 1229 Parascandola, A., 1947. I Fenomeni Bradisismici del Serapeo di Pozzuoli. Stabilimento Tipografico
1230 G. Genovese, Napoli.
1231
- 1232 Parmigiani, A., Huber, C., Bachmann O., 2014. Mush microphysics and the reactivation of crystal-
1233 rich magma reservoirs. *JGR*, <https://doi.org/10.1002/2014JB011124>
1234
- 1235 Pasquarè, G., Poli, S., Venzolli L., Zanchi A., 1988. Continental arc volcanism and tectonic setting
1236 in central Anatolia. *Tectonophysics*, 146, 217-230
- 1237 Rolandi, G., D'Alessio, G., Di Vito, M. (1985). Il sollevamento del suolo durante la fase preeruttiva
1238 del Monte Nuovo (Campi Flegrei). *Rend. Acc., Sc. Fis. e Mat. in Napoli*, 4, 52, 15 - 34
- 1239 Rolandi, G., Bellucci, F., Heitzler, M.T., Belkin, H.E., De Vivo, B., 2003. Tectonic controls on the
1240 genesis of the ignimbrites from the Campanian volcanic zone, southern Italy. In 'Ignimbrites of the
1241 Campanian Plain' Spec. Issue, B. De Vivo and R. Scandone Eds., *Mineralogy and Petrology*, 79, 3–
1242 31
- 1243 Rolandi, G., De Natale G., Kilburn, C.R.J. et al., 2020a. The 39 ka Campanian Ignimbrite eruption:
1244 new data on source area in the Campanian Plain,” in *Vesuvius, Campi Flegrei, and Campanian*
1245 *volcanism*, Chapt. 8, B. Vivo, H. E. Belkin, and G. Rolandi, Eds., pp. 175–205, Elsevier
- 1246 Rolandi, G., Di Lascio, M., Rolandi, R., 2020b. The Neapolitan Yellow Tuff eruption as the source
1247 of the Campi Flegrei caldera. in *Vesuvius, Campi Flegrei, and Campanian volcanism*, Chapt. 11, B.
1248 Vivo, H. E. Belkin, and G. Rolandi, Eds., pp. 273–296, Elsevier.
- 1249 Rosi, M., Sbrana, A., (Eds.) 1987. Phlegrean fields (Vol. 9). Consiglio nazionale delle ricerche.
1250
- 1251 Russo Mailer, C., 1979. La tradizione Medioevale dei bagni flegrei. *Puteoli, studi di storia antica*, III,
1252 141-153
- 1253 Sabetta, F., Paciello, A., 1995. Valutazione della pericolosità sismica. *La geologia di Roma- Memorie*
1254 *descrittive della carta geologica d'Italia*.



- 1255 Sacchi, M., Pepe, F., Corradino, M., Insinga, D.D., Molisso, F., Lubritto C., 2014. The Neapolitan
1256 Yellow Tuff caldera offshore the Campi Flegrei: stratal architecture and kinematic reconstruction
1257 during the last 15 ky. *Mar. Geol.* 354, 5-33
- 1258 Sacchi, M., Passaro, S., Molisso, F., Matano, F., Steinmann, L., Spiess, V., Pepe, F., Corradino, M.,
1259 Caccavale, M., Tamburrino, S., Esposito, G., Vallefucio, M., Ventura, G., 2020a. The Holocene
1260 marine record of unrest, volcanism, and hydrothermal activity of Campi Flegrei and Somma
1261 Vesuvius. In: B. De Vivo, H.E. Belkin and G. Rolandi (Eds.) *Vesuvius, Campi Flegrei, and*
1262 *Campanian Volcanism*, Elsevier Inc., Amsterdam, 435-469;
1263 <https://doi.org/10.1144/GSL.SP.2006.269.01.0310.1016/B978-0-12-816454-9.00016-X>.
1264
- 1265 Sacchi, M., Matano, F., Molisso, F., Passaro, S., Caccavale, M., Di Martino, G., Guarino, A., Innangi,
1266 S., Tamburrino, S., Tonielli, R., Vallefucio, M., 2020b. Geological framework of the Bagnoli–
1267 Coroglio coastal zone and continental shelf, Pozzuoli (Napoli) Bay. *Chem. Ecol.*, 36, 529–549.
1268
- 1269 Scafetta, N., Mazzarella, A., 2021. On the rainfall triggering of Phlegraean Fields volcanic tremors.
1270 *Watermark*, 13, 2.
- 1271 Scandone, R., D’Amato, J., Giacomelli, L., 2010. The relevance of the 1198 eruption of Solfatara in
1272 the Phlegraean Fields (Campi Flegrei) as revealed by medieval manuscripts and historical sources.
1273 *Journ. Volcanol. Geoth. Res.*, 189, 1–2, 202-206.
- 1274 Scarpa, R., Bianco, F., Capuano, P., Castellano, M., D’Auria, L., Di Lieto, B., Romano, P., 2022.
1275 Historic unrest of the Campi Flegrei caldera. In *Campi Flegrei. A Restless Caldera in A Densely*
1276 *Populated Area* (eds Orsi, G., D’Antonio, M. & Civetta, L.), 257–282.
- 1277 Selva, J., Orsi, G., Di Vito, M., Marzocchi, W., Sandri, L., 2011. Probability hazard map for future
1278 vent opening at the Campi Flegrei caldera, Italy. *Bull. Volcanol.*, [https://doi.org/10.1007/s00445-011-](https://doi.org/10.1007/s00445-011-1279-0528-2)
1279 0528-2 1-0528-2.
- 1280 Somma, R., Iuliano, S., Matano, F., Molisso, F., Passaro, S., Sacchi M., Troise C., De Natale, G.,
1281 2016. High-resolution morphobathymetry of Pozzuoli Bay, southern Italy. *Journ. Maps*, 12, 222–
1282 230, <https://doi.org/10.1080/17445647.2014.1001800>.
- 1283 Soricelli, G., 2007. *Comunità orientali a Puteoli*. Press. Univers., Rennes, 129-144,
1284 <https://doi.org/10.4000/books.pur.6714>



- 1285 Sparks, S.R.J., Sigurdsson, H., Wilson, L., 1977. Magma mixing: a mechanism for triggering acid
1286 explosive eruptions. *Nature*, 267, 315–318
- 1287 Shelly, D., Hurwitz, S., 2022. Yellowstone caldera chronicles, September 5. Yellowstone Volcano
1288 Observatory, USGS ([https://www.usgs.gov/observatories/yvo/news/water-released-crystallizing-](https://www.usgs.gov/observatories/yvo/news/water-released-crystallizing-magma-can-trigger-earthquakes-yellowstone)
1289 [magma-can-trigger-earthquakes-yellowstone](https://www.usgs.gov/observatories/yvo/news/water-released-crystallizing-magma-can-trigger-earthquakes-yellowstone))
- 1290 Smith, V.C., Isaia, R., Pearce, N.J.G., 2011. Tephrostratigraphy and glass compositions of post-15 kyr
1291 Campi Flegrei eruptions: implications for eruption history and chronostratigraphic markers. *Quat.*
1292 *Sci. Rev.* 30, 3638–3660
- 1293
- 1294 Steinmann, L., Spiess, V., Sacchi, M., 2016. The Campi Flegrei caldera (Italy): Formation and
1295 evolution in interplay with sea-level variations since the Campanian Ignimbrite eruption at 39 ka.
1296 *Journ. Volcanol. Geoth. Res.*, 327, 361-374
- 1297
- 1298 Strabone, 1 century BC - 1 century AD. *Rerum Geogr.*, book V, cap. 4-5
- 1299
- 1300 Talavera Montes, A.J., 2021. Eruzioni, sismi e bradisismo nei Campi Flegrei in epoca romana tra
1301 fonti storiche ed evidenze archeologiche e geologiche. In: *Living with Seismic Phenomena in the*
1302 *Mediterranean and Beyond between Antiquity and the Middle Ages*, Proceedings of Cascia (25-26
1303 October, 2019) and Le Mans (2-3 June, 2021) Conferences. Edited by Compatangelo Soussignan R.
1304
- 1305 Troise, C., De Natale, G., Schiavone, R., Somma, R., Moretti, R., 2019. The Campi Flegrei caldera
1306 unrest: Discriminating magma intrusions from hydrothermal effects and implications for possible
1307 evolution. *Earth Sci. Rev.*, 188, 108-122, <https://doi.org/10.1016/j.earscirev.2018.11.007>.
- 1308
- 1309 Troise, C., Pingue, F., De Natale, G., 2003. Coulomb stress changes at calderas: modeling the
1310 seismicity of Campi Flegrei (Southern Italy). *J. Geophys. Res.*, 108, B6, 2292,
1311 <https://doi.org/10.1029/2002JB002006>
- 1312
- 1313 Vanorio, T., Prasad, M., Patella, D., Nur, A., 2002. Ultrasonic velocity measurements in volcanic
1314 rocks: Correlation with microtexture. *Geophys. Journ. Intern.*, 149, 1, 22-36,
1315 <https://doi.org/10.1046/j.0956-540x.2001.01580.x>
- 1316



- 1317 Vanorio, T., Virieux, J., Capuano, P., Russo, G., 2005. Threedimensional seismic tomography from
1318 P wave and S wave microearthquake travel times and rock physics characterization of the Campi
1319 Flegrei Caldera. *J. Geophys. Res.*, 110, 1-14
1320
- 1321 Vanorio, T., Kanitpanyacharoen, W., 2015. Rock physics of fibrous rocks akin to Roman concrete
1322 explains uplifts at Campi Flegrei. *Science*, 349, 617–621
1323
- 1324 Varriale, I., 2004. Costa Flegrea ed attività bradisismica dall'antichità ad oggi. In *Rotte e Porti del*
1325 *Mediterraneo dopo la caduta dell'Impero Romano d'Occidente. IV seminario*, Genova 18-19 Luglio.
1326 De Maria L. and Turchetti R. Eds.
1327
- 1328 Vinciguerra, S., Trovato, C., Meredith, P.G, Benson, P.M., Troise, C., De Natale, G., 2006.
1329 Understanding the Seismic Velocity Structure of Campi Flegrei Caldera (Italy): From the Laboratory
1330 to the Field Scale. *Pure appl. geophys.*, 163, 2205–2221, <https://doi.org/10.1007/s00024-006-0118-y>
1331
- 1332 Wohletz, K.H., Zimanowski, B., Büttner, B.R., 2013. Magma-water interactions. in *Modeling*
1333 *Volcanic Processes: The Physics and Mathematics of Volcanism* (Fagents, S.A., Gregg, T.K.P.,
1334 Lopes, R.M.C. eds.) 230–257. Cambridge University Press.
1335
- 1336 Woods, W., Cowan, A., 2009. Magma mixing triggered during volcanic eruption. *Earth and Planetary*
1337 *Science Letters*, 288, 1–2, 30, 132-137
- 1338 Woo, J.Y.L., Kilburn, C.R.J., 2010. Intrusion and deformation at Campi Flegrei, southern Italy: Sills,
1339 dikes, and regional extension. *J. Geophys. Res.*, 115, B12210
1340
- 1341 Wunderman, R. ed., 2000. Global volcanism Program. Report on Hekla (Iceland). *Bulletin of global*
1342 *volcanism network*, 25:2. Smithsonian Institution. [https:// doi org/10.5470/si](https://doi.org/10.5470/si).
1343
1344
1345
1346
1347

1348

Historical supplementary material

1349

1350

Appendix 1 - Evolution of the vertical movements involving the Via Herculea



1351

1352 The following notes refer to the diagram represented in Fig. 3, reporting at each point the historical information
1353 related to ground deformation in the Averno area:

1354

1355 **1-** The shoreline between the cities of Baia and Pozzuoli took on a new conformation with the natural building
1356 of a sandy coastal bar after the eruptions of Averno and Capo Miseno (5 - 3.7 ka), the last of the second post-
1357 calderic cycle. We remember that the name *Averno* derived from the Greek *Aornon*, that is *place without*
1358 *birds*, in reference to the presence of post-volcanic sulphurous fumes that caused the death of the birds that
1359 flew over the waters. The dark and gloomy appearance of the landscape led the ancients to consider it the
1360 entrance to Hades, as reported by Virgil (Aeneid, VI, vv 350).

1361 We do not know precisely the time of formation of the bar structure; we can only hypothesize that it was
1362 probably positioned between the 18th and 17th centuries BC in the coastal stretch between the cities of Baia
1363 and Pozzuoli, with a height of about 6 m, like the other coastal bars formed more recently in nearby areas,
1364 where the seabed has a depth of about 6-7 m. The formation of the sea barrier blocked a portion of the sea
1365 inside the inlet, which took the shape of a lake (Fig. 2a and Fig. 4).

1366

1367 **2-** This point can be traced back, from a historical and chronological point of view, to the 8th century BC. In
1368 the diagram it is positioned at approximately 5 m above sea level, suggesting a subsidence of the coastal bar
1369 of about 2 m from the previous point. In fact, from a writing by Diodorus Siculus (Book IV) we know that:..
1370 *this dam was continually invaded and ruined by the stormy sea, which often made it impassable...* It is known
1371 from coastal dynamics studies that waves breaking against a dam, placed above a seabed 7 m deep, reach a
1372 height equal to 3/4 of the depth of the same seabed, in this case approximately 5 m, i.e., a height equal to the
1373 barrier above the sea level. Therefore, the via Herculea, hit by violent waves, constituted an impassable road
1374 for the inhabitants of Cuma to reach the lands they cultivated in the surroundings of Pozzuoli, which, starting
1375 from the 8th century, took the name of Via Herculea (Fig. 2b and Fig. 4). Finally, the hypothesis of a height
1376 of 5 m, as resulting from submersion started since the 17th century BC, seems likely.

1377

1378 **3- 4 -** The body of water formed by the coastal bar, in the 1st century BC, was owned by Sergio Orata. The
1379 lake, making generous profits from fish farming, was named "*Lucrino*", derived from the Latin *Lucrum* (profit)
1380 (Fig. 2c). The owner, around 60 BC, to protect his interests turned directly to the Roman Senate to have the
1381 Via Herculea repaired, because at that time, being at a height of about 2 m above sea level, it had almost been
1382 destroyed by the waves that crossed it, preventing him from practicing his lucrative fish farming business
1383 (point 3). The Senate appointed Julius Caesar, who in 59 BC built a breakwater barrier, located outside the
1384 dam towards the open sea (Opus Pilarum). He also ordered the installation of canals closed by opening
1385 platforms (Claustre). Julius Caesar's project defended the Via Herculea essentially from the horizontal force
1386 exerted by violent wave motion, not understanding the effect of subsidence. In 37 BC, general Agrippa, by
1387 order of Octavian, engaged in the naval war against Pompeo Sextus, chose the coastal sector between the lakes
1388 Lucrino and Avernus for the construction of a new military port system, called *Portus Julius*. A new main



1389 entrance was built, consisting of a canal with two long banks in ‘opus pilarum’, cutting and equipping the Via
1390 Herculea with a mobile bridge, to access its interior, while at the same time widening the narrow opening that
1391 connected the Averno and Lucrino lakes to allow access of large ships in the shipyard (Fig. 2c). Furthermore,
1392 Agrippa reinforced the Via Herculea and added piers, supported by orthogonal pillars and having also sensed
1393 a problem of subsidence,... *raised its level (Strabone, 1 century BC-1 century AD)* (point 4).

1394

1395 **5- 6** - The abandonment of Portus Julius by the Roman fleet, starting from 12 BC, as well as of the remaining
1396 part of Lake Lucrino, due to the impossibility of continuing fish farming, was the result of the continuing
1397 subsidence, which, according to Aucelli et al. (2020), between 37 BC and the beginning of the 1st century AD
1398 further accelerated.

1399 In the 5th century AD the dam, few meters above sea level (point 5), was also damaged by a violent sea storm.
1400 An attempt to restore the dam again was made by Theodoric, regent of the Ostrogothic kingdom in Italy from
1401 493 AD, who decided, in 496 AD, to repair the damage and probably also raised its level (*Cassiodorus, Varia,*
1402 *Book I*) (point 6). This can be also deduced from the fact that Lake Lucrino was still well identified in 522
1403 AD (G.C. Capaccio - Puteolana historia, in Parascandola 1943).

1404

1405 **7-8** - Around the second half of the 6th century (556 AD), some fishermen attempted to reactivate fish farming
1406 in Lake Lucrino, but the dam soon could not guarantee an adequate yield, because it had reached a height of
1407 just a few meters above sea level (point 7), not allowing fish farming (Parascandola, 1943).

1408 As we will show in Appendix-2, historical documents indicate that, at the lower city around Pozzuoli, the
1409 famous Serapeo (Macellum) began the phase of submersion below sea level in the 4th-5th century AD. At the
1410 area facing the Avernus, the above historical documents indicate that the submersion most likely occurred
1411 between the 6th and 7th centuries AD. This could be related to either height increasing interventions and /or
1412 to a lower speed of subsidence at the site of Via Herculea, as compared to the Serapeo.

1413

1414 **9** – In the 14th century we have evidence of the submersion through the writings of Petrarca and Boccaccio.
1415 Below we will report some sentences from the two poets, giving indications on the subsidence in this period
1416 (Parascandola 1943):

1417 - Petrarca, who lived in Naples in 1341, visited the coastal area of Avernus, (*...I then saw the places of*
1418 *Avernus and Lucrino..... and the superb road of Gaius Caligula now swallowed up by the waves..... Note*
1419 *that Opus Pilarum mistakenly believed to be the road of Caligula*). From this observation we deduce that
1420 Opus Pilarum was submerged in the 14th century (Fig. A1). From the same observation it further seems likely
1421 that, since the 4-5 m high pylons, submerged for a couple of metres, are not visible, and given the pylons were
1422 higher than Via Herculea of about 3 meters, the already submerged Via Herculea should have been submerged
1423 at that time for about 5-6 m.

1424 - Boccaccio came to Naples in 1348 and, after visiting the Averno area, he clearly expressed the concept,
1425 although indirectly, that Lake Lucrino was not recognized as it was invaded by the sea, mixing with the waters



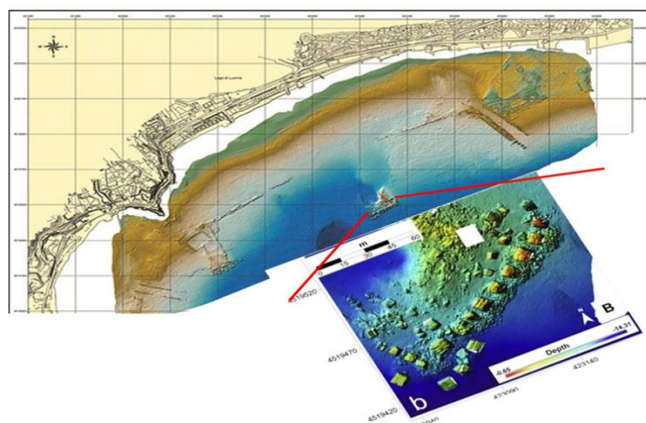
1426 of Avernus (...to Avernus, connected in ancient times with the nearby lake Lucrino where it recalls the
1427 waters of portus Iulius: Boccaccio, 1355-1373).

1428 Boccaccio noted that, since there was no barrier on the Via Herculea which formed the Lucrino, the rough sea
1429 even broke into Lake Averno. Therefore, we can undoubtedly say that in the 14th century via Herculea was
1430 completely submerged and Lake Lucrino disappeared because it was invaded by the sea.

1431

1432 **10** - As we will demonstrate later, in the 15th century the ground movements of the Campi Flegrei area changed
1433 from subsidence to uplift. The uplift began, the actual amount of which in the Averno area can be only given
1434 in an approximate but equally significant way, because it is ascertained, from the writings of all the chroniclers
1435 of the time (see Parascandola, 1943) that the Via Herculea did not re-emerge in this period (fig 2d). What is
1436 reported by the historian San Felice is almost common to all the chroniclers: *The sea had taken possession of*
1437 *Lucrino, so that the name could no longer be given to the ancient lake.*

1438



1439

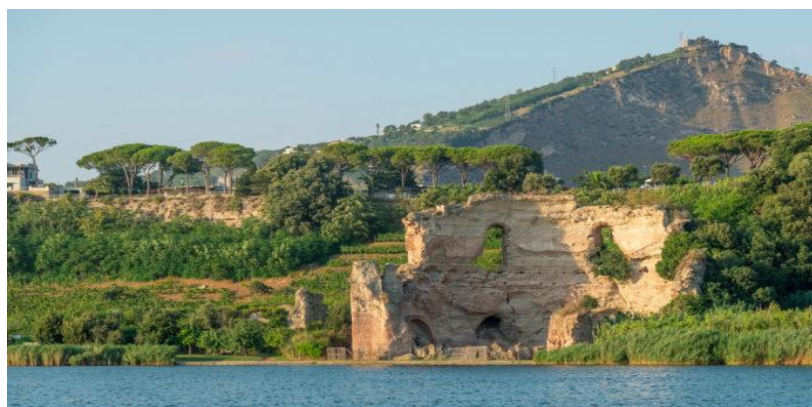
1440 **Fig. A1 - The remains of the Via Herculea currently located at 4-5m bsl, with the columns of Opus**
1441 **Pilarum approximately 300m away in the open sea. An enlargement of the structure of Opus Pilarum is**
1442 **also reported**

1443 Shortly before the eruption, the general caldera uplift was also accompanied by a localized uplift of the area
1444 where Monte Nuovo would have risen shortly after, in 1538, located in close contact with the Lucrino basin
1445 (Fig. 2d). Such a local uplift was estimated at about 7 m (Parascandola, 1943), so the Via Herculea would
1446 certainly have emerged if it had been close to the sea surface at the end of the 15th century. A significantly
1447 larger uplift, of 19 m as hypothesized by Di Vito et al (2016), can be certainly ruled out from the observation
1448 that Via Herculea did not reemerge.

1449 The topic of the local uplift before eruption is relevant, so we insist on other aspects linked to the entire area
1450 buried by the products of 1538 Monte Nuovo eruption. Until a short time before the eruptive event, two small
1451 tuff hills, called *Montagnella* and *Monticello del Pericolo* (Parascandola, 1936), overlooked the Averno Bay,



1452 above which the *village of Tripergole* extended. This village, thanks to the Angevins, developed with the
1453 construction of a hospital with 30 beds, to access the numerous springs and thermal facilities available to the
1454 hospitalized patients, with an adjoining pharmacy. Ancient buildings used for thermal baths (*Trugli*) present
1455 in the Tripergole area were highly compromised between the end of the 15th century and the beginning of the
1456 16th, when the Pozzuoli area was hit by major earthquakes. The earthquakes caused extensive damage to the
1457 thermal health and ecclesiastical buildings of Tripergole, but not so devastating than expected if a ground uplift
1458 about 20 m high would have occurred. Also the so-called *Temple of Apollo*, still present along the north-
1459 eastern bank of the Averno lake (Fig. A2), testifies against a so large and sudden uplift. The structure is an
1460 imposing building identified as a grandiose thermal room, covered by a dome, now partly collapsed, which
1461 measured approximately 38 metres in diameter, built in the 1st century AD to exploit a series of hydrothermal
1462 springs along the eastern side of Avernus, then expanded with the large octagonal hall (the one that is still
1463 visible) in the following century. This structure was identified by Biondo da Forlì as the bathroom of Cicero
1464 (Lanzarin, 2021), that, due to its particular location protected by the Averno crater belt, was not involved in
1465 the burial of the *Monticello del Pericolo*, the *Montagnella* and the village of *Tripergole*, with its renowned
1466 thermal baths.
1467



1468
1469 **Fig. A2 – The so-called Temple of Apollo on the east bank of the Avernus. You can see the remains of a**
1470 **circular building with a "cap" vault, which later collapsed, typical of a "Truglio", i.e. a spa building**
1471 **(internet source)**

1472

1473 **Appendix 2 - Evolution of the ground movements involving the Pozzuoli area**

1474

1475 Phases of submersion during the Greek age have been detected in the Pozzuoli area by Gauthier (1912),
1476 specifically in the eastern sector of Agnano. The author discovered Greek walls beneath the ruins of Roman
1477 baths which were restored in the 6th century AD. These, in turn, underlie lacustrine sediments that filled an
1478 ancient lake originally existing within the Agnano crater. However, the most evident subsidence phases have
1479 been recorded since Roman times, by the structures of the so-called Temple of Serapis in Pozzuoli. Built in



1480 the 2nd century AD and restored and completed in the 3rd century AD, during the Severan era, this structure
1481 exhibits the typical architecture of a Roman market ("Macellum").

1482 To determine whether the construction preceding the 2nd century AD had a connection with a temple, we must
1483 go back to 105 BC, when a contract was stipulated between the municipality of Pozzuoli and a college of
1484 builders for repairs of public buildings (lex parieti faciundo). Among these was the Ades Serapis (Parascandola
1485 1947), indicating that a temple dedicated to Serapis, (an Alexandrian deity often regarded as protector of
1486 merchants and sailors) existed during this period. By the end of the 2nd century BC, the cult of Serapis had
1487 spread throughout the Mediterranean and its sanctuaries, as well as those of other Egyptian deities, were
1488 frequented by Roman-Italics. It is probable, therefore, that the introduction of the cult of Serapis in Puteoli is
1489 related to the presence of an Egyptian community in the Puteolan port (Soricelli 2007). It is important to try to
1490 establish the relationships between this building and the Macellum built later, specifically whether the Ades
1491 Serapis could have an ancestral link with a more recent cult building, that was then transformed into a typical
1492 Roman market. This relationship is suggested by the discovery of a statue of Jupiter Serapis during the
1493 excavations of the Macellum in 1750 (see below). However, data reconstructed by Amato and Gialanella
1494 (2013; Fig.3), indicate that the first floor present in the substrate below the Macellum dates from the Flavian
1495 period (69 -96 AD). The finds in the reworked pyroclastic materials which are 4 meters thick below the first
1496 floor indicate a chronological interval between the end of the Republic and the beginning of the Empire (44
1497 BC - 14 AD). This suggests that the Ades Serapis was likely built in a different position from the macellum,
1498 with which it therefore has no ties. The architectural elements of Macellum are part of the restoration works
1499 carried out on the Serapeo during the Severan Age (194 - 235 AD), with the installation of the 4th floor around
1500 230 AD, located approximately 2 m above the 3rd floor. The existing structure (Fig. 6), still present in the
1501 same area today, provides important evidence for reconstructing the ground movements. These movements
1502 can be identified in:

1503 *The marble floor of the macellum (4th floor; see also Fig. A3b);

1504 * The height of the three columns of the pronaos (12.70 m high, with the first 6.2 m displaying a 2.70m band
1505 perforated by lithophagus colonies (Fig. A3).

1506 The historical information about the ground movements, is schematized in Fig. 6 of the main text, as follows:

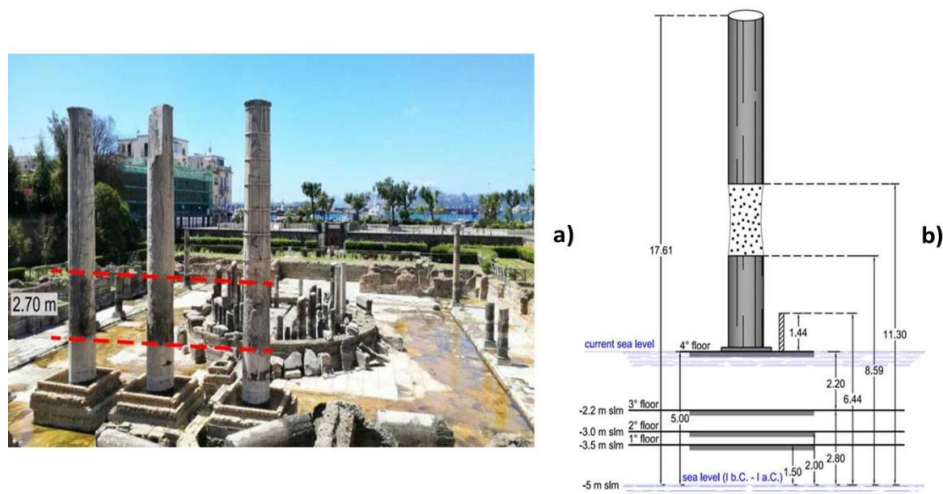
1507 **1** - In the 2nd century AD the 3rd floor of the Serapeum reached approximately 1m above sea level. It was
1508 sporadically invaded by the sea, to the point that, it was considered appropriate to build a 4th floor in 230 AD,
1509 located at 2m above sea level.

1510

1511 **2** - The flooding progressively affected the coast, leading to the transfer of ships from the port of Puteoli to
1512 Constantinople in 325-330 AD (Gianfrotta 1993). It is important to highlight that the 4th floor was invaded
1513 by the sea in 394 AD. The bank was restored on the left side and the right side of the macellum, in the area
1514 where structures functional to the port and the emporium were located, and to protect it from the sea waves
1515 with the construction of coastal embankments. These important works were supervised by the Campanian
1516 Consul Valerius Hermonius Maximus (Camodeca 1987, Caruso 2004).



1517



1518

1519

Fig. A3 – a) Macellum showing pronao columns, b) Floors underlying columns

1520

1521 **3** - In the 6th-7th century, the citizens who had completely depopulated the lower part of Pozzuoli felt the need
 1522 to take refuge in a sort of fortified citadel (castrum), equipped with a drawbridge, giving rise to the Acropolis
 1523 of the Rione Terra (Varriale 2004).

1524

1525 **4** - In the 9-10th century, according to Parascandola (1943), the maximum submersion of the 4th floor of the
 1526 Serapeum occurred. Due to the subsidence of the Pozzuoli area, between the 8th and 10th centuries, the Agnano
 1527 Plain, immediately east of Pozzuoli, was invaded by water for the stagnation of thermal and rainwater,
 1528 transforming it into a lake (Anneccchino, 1931).

1529

1530 **5 -7** - In such a context, the most critical periods of the submersion phase occurred. The sea increasingly
 1531 surrounded the Rione Terra, that appeared like a medieval village, with a drawbridge at the entrance to the
 1532 cliff. The same context was depicted in the 11th century by the Arab geographer *Idrisi* in his *Opus*
 1533 *Geographicum*, describing Pozzuoli as a "castle" (Varriale, 2004).

1534 In the 12th century subsidence was still active. A writing deriving from an account of Benjamin ben Yonah
 1535 de Tudela who, visiting the Jewish communities of the Mediterranean, passing through Pozzuoli, described:
 1536 *turres et fora in aqua demersa quae in media quondam fuerant* (Russo Mailer C. 1979, Caruso 2004). The
 1537 Pozzuoli district continued to subside in the 13th century, as can be deduced from an account written in 1251
 1538 by the historian Niccolò Jamsilla (*Historia de rebus gestis Frederici II imperatoris eisque filorum*
 1539 *Corradiet Manfredi Apuliae et Siciliae regnum*) describes the places between Agnano and Pozzuoli as
 1540 follows: *...videlicet Putheolum mari mantibusque inaccessibilius circumquaque conclusum...*(Fuiano
 1541 1951).



1542 In essence, what was observed by the Arab geographer Idris in the 11th century, was also written by the
1543 historian Jamsilla in 1251, confirming that Rione Terra “was *an unapproachable mountain completely*
1544 *surrounded by the sea*”. This highlights that, over more than 3 centuries, the sea level rose due to subsidence
1545 of the tuffaceous walls of the Rione Terra.

1546

1547 **8** – Further eyewitness accounts from by Boccacio, who lived in Naples between 1327 and 1341, reported that
1548 a fisherman's wharf in the Bay of Pozzuoli became completely submerged (Mancusi, 1987). This document
1549 supports the description of the lower part of the city being completely submerged.

1550

1551 **9** – A gouache from 1430, known as *Bagno del Cantariello*, part of the famous Balneis Puteolanis of the
1552 Edinburgh Codex (Di Bonito & Giamminelli, 1992) indicates the complete submergence of the 4th floor of
1553 the Serapeum by at least 10 meters. (Fig. 7). This context is supported by a description from 1441 indicating
1554 that in 1441 “*the sea covered the littoral plain, today called Starza*” (De Jorio, 1820; Dvorak and
1555 Mastrolorenzo, 1991) (see Fig. 8).

1556 For a more precise description of this morphological context, it is useful to refer to the excavation of the
1557 Serapeum carried out in 1750, when this monument was freed from the blanket of sediments that buried it (see
1558 Fig. 12), made up of approximately 8 m of filling sediments, plus two meters of deposits from the pyroclastic
1559 flow of the M. Nuovo eruption. By replacing the latter materials with the approximately 2 m blade of sea water
1560 in the 1430 scenario (Fig. 7c), we arrive at the landscape picture in Fig. 7a, exemplified in Fig. 8d.

1561

1562

1563

1564

1565

1566

1567

1568

1569

1570

1571

1572

1573

1574

1575

1576

1577